Predictive Coding, Variational Autoencoders, and Biological Connections

Joseph Marino[1]

josephmarino@deepmind.com
Computation & Neural Systems,
California Institute of Technology,
Pasadena, CA 91125, USA

Abstract

This paper reviews predictive coding, from theoretical neuroscience, and variational autoencoders, from machine learning, identifying the common origin and mathematical framework underlying both areas. As each area is prominent within its respective field, more firmly connecting these areas could prove useful in the dialogue between neuroscience and machine learning. After reviewing each area, we discuss two possible correspondences implied by this perspective: cortical pyramidal dendrites as analogous to (non-linear) deep networks and lateral inhibition as analogous to normalizing flows. These connections may provide new directions for further investigations in each field.

1   Introduction

1.1   Cybernetics

Machine learning and theoretical neuroscience once overlapped under the field of cybernetics (Wiener, 1948; Ashby, 1956). Within this field, perception and control, both in biological and non-biological systems, were formulated in terms of negative feedback and feedforward processes. Negative feedback attempts to minimize error signals by *feed*ing the errors *back* into the system, whereas feedforward processing attempts to preemptively reduce error through prediction. Cybernetics formalized these techniques using probabilistic models, which estimate the likelihood of random outcomes, and variational calculus, a technique for estimating functions, particularly probability distributions (Wiener, 1948). This resulted in the first computational models of neuron function and learning (McCulloch & Pitts, 1943; Rosenblatt, 1958; Widrow & Hoff, 1960), a formal definition of information (Wiener, 1942; Shannon, 1948) (with connections to neural systems (Barlow, 1961)), and algorithms

---

[1]Now at DeepMind, London, UK.

for negative feedback perception and control (MacKay, 1956; Kalman, 1960). Yet, with advances in these directions (see Prieto et al. (2016) and references therein), the cohesion of cybernetics diminished, with the new ideas taking root in theoretical neuroscience, machine learning, control theory, etc.

1.2   Neuroscience & Machine Learning: Convergence & Divergence

A renewed dialogue between neuroscience and machine learning formed in the 1980s–1990s. Neuroscientists, bolstered by new physiological and functional analyses, began making traction in studying neural systems in probabilistic and information-theoretic terms (Laughlin, 1981; Srinivasan et al., 1982; Barlow, 1989; Bialek et al., 1991). In machine learning, improvements in probabilistic modeling (Pearl, 1986) and artificial neural networks (Rumelhart et al., 1986) combined with ideas from statistical mechanics (Hopfield, 1982; Ackley et al., 1985) to yield new classes of models and training techniques. This convergence of ideas, primarily centered around perception, resulted in new theories of neural processing and improvements in their mathematical underpinnings.

In particular, the notion of *predictive coding* emerged within neuroscience (Srinivasan et al., 1982; Rao & Ballard, 1999). In its most general form, predictive coding postulates that neural circuits are engaged in estimating probabilistic models of other neural activity and sensory inputs, with feedback and feedforward processes playing a central role. These models were initially formulated in early sensory areas, e.g., retina (Srinivasan et al., 1982) and thalamus (Dong & Atick, 1995), using feedforward processes to predict future neural activity. Similar notions were extended to higher-level sensory processing in neocortex by David Mumford (Mumford, 1991, 1992). Top-down neural projections (from higher-level to lower-level sensory areas) were hypothesized to convey sensory predictions, whereas bottom-up neural projections were hypothesized to convey prediction errors. Through negative feedback, these errors then updated state estimates. These ideas were formalized by Rao & Ballard (1999), formulating a simplified artificial neural network model of images, reminiscent of a Kalman filter (Kalman, 1960).

Feedback and feedforward processes also featured prominently in machine learning. Indeed, the primary training algorithm for artificial neural networks, backpropagation (Rumelhart et al., 1986), literally *feeds* (propagates) the output prediction errors *back* through the network, i.e., negative feedback. During this period, the technique of variational inference was rediscovered within machine learning (Hinton & Van Camp, 1993; Neal & Hinton, 1998), recasting probabilistic inference using variational calculus. This technique proved essential in formulating the Helmholtz machine (Dayan et al., 1995; Dayan & Hinton, 1996), a hierarchical unsupervised probabilistic model parameterized by artificial neural networks. Similar advances were made in autoregressive probabilistic models (Frey et al., 1996; Bengio & Bengio, 2000), using artificial neural networks to form sequential feedforward predictions, as well as new classes of invertible probabilistic models (Comon, 1994; Parra et al., 1995; Deco & Brauer, 1995; Bell & Sejnowski, 1997).

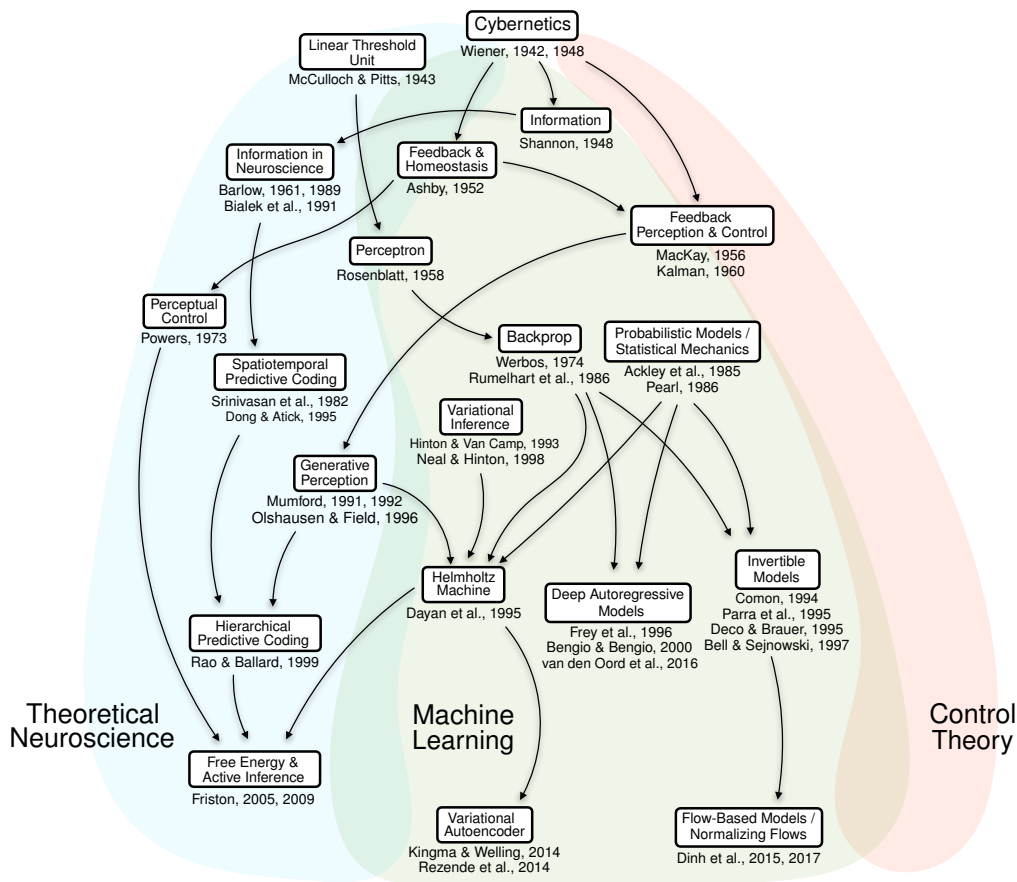These new ideas regarding variational inference and probabilistic models, particularly

Figure 1: **Concept Overview**. Cybernetics influenced the areas that became theoretical neuroscience and machine learning, resulting in shared mathematical concepts. This paper explores the connections between predictive coding, from theoretical neuroscience, and variational autoencoders, from machine learning.

the Helmholtz machine (Dayan et al., 1995), influenced predictive coding. Specifically, Karl Friston utilized variational inference to formulate hierarchical dynamical models of neocortex (Friston, 2005, 2008a). In line with Mumford (1992), these models contain multiple levels, with each level attempting to predict its future activity (feedforward) as well as lower-level activity, closer to the input data. Prediction errors across levels facilitate updating higher-level estimates (negative feedback). Such models have incorporated many biological aspects, including local learning rules (Friston, 2005) and attention (Spratling, 2008; Feldman & Friston, 2010; Kanai et al., 2015), and have been compared with neural circuits (Bastos et al., 2012; Keller & Mrsic-Flogel, 2018; Walsh et al., 2020). While predictive coding and other Bayesian brain theories are increasingly popular (Doya et al., 2007; Friston, 2009; Clark, 2013), validating these models is hampered by the difficulty of distinguishing between specific design choices and general theoretical claims (Gershman,

2019). Further, a large gap remains between the simplified implementations of these models and the complexity of neural systems.

Progress in machine learning picked up in the early 2010s, with advances in parallel computing as well as standardized datasets (Deng et al., 2009). In this era of *deep learning* (LeCun et al., 2015; Schmidhuber, 2015), i.e., artificial neural networks with multiple layers, a flourishing of ideas emerged around probabilistic modeling. Building off of previous work, more expressive classes of deep hierarchical (Gregor et al., 2014; Mnih & Gregor, 2014; Kingma & Welling, 2014; Rezende et al., 2014), autoregressive (Uria et al., 2014; van den Oord, Kalchbrenner, & Kavukcuoglu, 2016), and invertible (Dinh et al., 2015, 2017) probabilistic models were developed. Of particular importance is a model class known as *variational autoencoders* (VAEs) (Kingma & Welling, 2014; Rezende et al., 2014), a relative of the Helmholtz machine, which closely resembles hierarchical predictive coding. Unfortunately, despite this similarity, the machine learning community remains largely oblivious to the progress in predictive coding and vice versa.

1.3 Connecting Predictive Coding and VAEs

This paper aims to bridge the divide between predictive coding and VAEs. While the present work provides unique contributions, it is inspired by previous works at this intersection. In particular, van den Broeke (2016) outlines hierarchical probabilistic models in predictive coding and machine learning. Likewise, Lotter et al. (2017, 2018) implement predictive coding techniques in deep probabilistic models, comparing these models with neural phenomena.

After reviewing background mathematical concepts (Sec. 2), we discuss the basic formulations of predictive coding (Sec. 3) and variational autoencoders (Sec. 4), identifying commonalities in their model formulations and inference techniques (Sec. 5). Based on these connections, in Sec. 6, we discuss two possible correspondences between machine learning and neuroscience seemingly suggested by this perspective:

- **dendrites of pyramidal neurons & deep artificial networks**, affirming a more nuanced perspective over the analogy of biological and artificial neurons, and

- **lateral inhibition & normalizing flows**, providing a more general framework for normalization.

Like the works of van den Broeke (2016) and Lotter et al. (2017, 2018), we hope that these connections will inspire future research in exploring this promising direction.

2 Background

2.1 Maximum Log-Likelihood

Consider a random variable, $\mathbf{x} \in \mathbb{R}^M$, with a corresponding distribution, $p_{\text{data}}(\mathbf{x})$, defining the probability of observing each possible value. This distribution is the result of an

underlying data generating process, e.g., the emission and scattering of photons. While we do not have direct access to p_{data}, we can sample observations, $\mathbf{x} \sim p_{\text{data}}(\mathbf{x})$, yielding an empirical distribution, $\widehat{p}_{\text{data}}(\mathbf{x})$. Often, we wish to model p_{data}, e.g., for prediction or compression. We refer to this model as $p_\theta(\mathbf{x})$, with parameters θ. Estimating the model parameters involves maximizing the log-likelihood of data samples under the model's distribution:

$$\theta^* \leftarrow \arg \max_\theta \mathbb{E}_{\mathbf{x} \sim p_{\text{data}}(\mathbf{x})} \left[\log p_\theta(\mathbf{x}) \right]. \tag{1}$$

This is the *maximum log-likelihood* objective, which is found throughout machine learning and probabilistic modeling (Murphy, 2012). In practice, we do not have access to $p_{\text{data}}(\mathbf{x})$ and instead approximate the objective using data samples, i.e., using $\widehat{p}_{\text{data}}(\mathbf{x})$.

2.2 Probabilistic Models

2.2.1 Dependency Structure

A probabilistic model includes the dependency structure (Sec. 2.2.1) and the parameterization of these dependencies (Sec. 2.2.2). The dependency structure is the set of conditional dependencies between variables. One common form is given by **autoregressive models** (Frey et al., 1996; Bengio & Bengio, 2000), which use the chain rule of probability:

$$p_\theta(\mathbf{x}) = \prod_{j=1}^{M} p_\theta(x_j | x_{<j}). \tag{2}$$

By inducing an ordering over the M dimensions of $\mathbf{x}$, we can factor the joint distribution, $p_\theta(\mathbf{x})$, into a product of M conditional distributions, each conditioned on the previous dimensions, $x_{<j}$. A natural use-case arises in modeling sequential data, where time provides an ordering over a sequence of T variables, $\mathbf{x}_{1:T}$:

$$p_\theta(\mathbf{x}_{1:T}) = \prod_{t=1}^{T} p_\theta(\mathbf{x}_t | \mathbf{x}_{<t}). \tag{3}$$

Autoregressive models are "fully-visible" models (Frey et al., 1996), as dependencies are only modeled between observed variables. However, we can also introduce *latent variables*, $\mathbf{z}$. Formally, a **latent variable model** is defined by the joint distribution

$$p_\theta(\mathbf{x}, \mathbf{z}) = p_\theta(\mathbf{x}|\mathbf{z})p_\theta(\mathbf{z}), \tag{4}$$

where $p_\theta(\mathbf{x}|\mathbf{z})$ is the *conditional likelihood* and $p_\theta(\mathbf{z})$ is the *prior*. Introducing latent variables is one of, if not, *the* primary technique for increasing the flexibility of a model, as evaluating the likelihood now requires marginalizing over the latent variables:

$$p_\theta(\mathbf{x}) = \mathbb{E}_{\mathbf{z} \sim p_\theta(\mathbf{z})} \left[p_\theta(\mathbf{x}|\mathbf{z}) \right]. \tag{5}$$
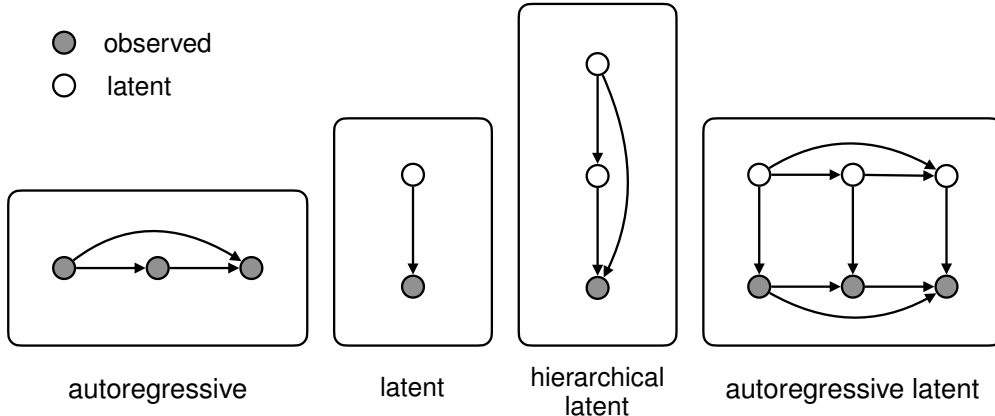
Figure 2: **Dependency Structures**. Each diagram shows a directed graphical model. Nodes represent random variables, and arrows represent dependencies. The main forms of dependency structure are autoregressive (Eq. 2) and latent variable models (Eq. 4). These structures can be combined in various ways (Eqs. 7 & 8).

Thus, $p_\theta(\mathbf{x})$ is a *mixture* distribution, with each component, $p_\theta(\mathbf{x}|\mathbf{z})$, weighted according to $p_\theta(\mathbf{z})$. Even when $p_\theta(\mathbf{x}|\mathbf{z})$ takes a simple distribution form, such as Gaussian, $p_\theta(\mathbf{x})$ can take on flexible forms. In this way, $\mathbf{z}$ can capture complex dependencies in $\mathbf{x}$.

However, increased flexibility comes with increased computational cost. In general, marginalizing over $\mathbf{z}$ is not tractable. This requires us to 1) adopt approximations, discussed in Sec. 2.3, or 2) restrict the model to ensure tractable evaluation of $p_\theta(\mathbf{x})$ (Eq. 5). The latter approach is taken by **flow-based latent variable models** (Tabak & Turner, 2013; Rippel & Adams, 2013; Dinh et al., 2015), defining the dependency between $\mathbf{x}$ and $\mathbf{z}$ via an invertible transform, $\mathbf{x} = f_\theta(\mathbf{z})$ and $\mathbf{z} = f_\theta^{-1}(\mathbf{x})$. With a prior or *base distribution*, $p_\theta(\mathbf{z})$, we can express $p_\theta(\mathbf{x})$ using the *change of variables formula*:

$$p_\theta(\mathbf{x}) = p_\theta(\mathbf{z}) \left| \det\left(\frac{\partial \mathbf{x}}{\partial \mathbf{z}} \right) \right|^{-1}, \tag{6}$$

where $\frac{\partial \mathbf{x}}{\partial \mathbf{z}}$ is the Jacobian of the transform and $\det(\cdot)$ denotes matrix determinant. The term $\left| \det\left(\frac{\partial \mathbf{x}}{\partial \mathbf{z}} \right) \right|^{-1}$ is the local scaling of space when moving from $\mathbf{z}$ to $\mathbf{x}$, conserving probability mass. Flow-based models, also referred to as *normalizing flows* (Rezende & Mohamed, 2015), are the basis of independent components analysis (ICA) (Comon, 1994; Bell & Sejnowski, 1997; Hyvärinen & Oja, 2000) and non-linear generalizations (Chen & Gopinath, 2001; Laparra et al., 2011). These models provide a general-purpose mechanism for adding and removing dependencies between variables, i.e., normalization.[2] Yet, while flow-based

---

[2]Formally, we refer to normalization as one or more steps of a process transforming the data density into a standard Gaussian (i.e., Normal), which is equivalent to ICA (Hyvärinen & Oja, 2000). This is a form of redundancy reduction, removing statistical dependencies between data dimensions.

models avoid marginalization, their requirement of invertibility can be overly restrictive (Cornish et al., 2020).

We have presented autoregression and latent variables separately, however, these techniques can be combined. For instance, *hierarchical latent variable models* (Dayan et al., 1995) incorporate autoregressive dependencies between latent variables. Considering L levels of latent variables, $\mathbf{z}^{1:L} = \left[\mathbf{z}^1, \ldots, \mathbf{z}^L \right]$, we can express the joint distribution as

$$p_\theta(\mathbf{x}, \mathbf{z}^{1:L}) = p_\theta(\mathbf{x}|\mathbf{z}^{1:L}) \prod_{\ell=1}^{L} p_\theta(\mathbf{z}^\ell|\mathbf{z}^{\ell+1:L}). \tag{7}$$

We can also incorporate latent variables within sequential (autoregressive) models, giving rise to *sequential latent variable models*. Considering a single level of latent variables in a corresponding sequence, $\mathbf{z}_{1:T}$, we have the following joint distribution:

$$p_\theta(\mathbf{x}_{1:T}, \mathbf{z}_{1:T}) = \prod_{t=1}^{T} p_\theta(\mathbf{x}_t|\mathbf{x}_{<t}, \mathbf{z}_{\leq t}) p_\theta(\mathbf{z}_t|\mathbf{x}_{<t}, \mathbf{z}_{<t}). \tag{8}$$

This encompasses special cases, such as hidden Markov models or linear state-space models (Murphy, 2012). There are a variety of other ways to combine autoregression and latent variables (Gulrajani et al., 2017; Razavi et al., 2019). In some cases, autoregressive and flow-based latent variable models are even equivalent (Kingma et al., 2016).

2.2.2 Parameterizing the Model

The distributions defining probabilistic dependencies are functions. In this section, we discuss forms that these functions may take. The canonical example is the Gaussian (or Normal) distribution, $\mathcal{N}(x; \mu, \sigma^2)$, which is defined by a mean, μ, and variance, σ^2. This can be extended to the multivariate setting, where $\mathbf{x} \in \mathbb{R}^M$ is modeled with a mean vector, $\boldsymbol{\mu}$, and covariance matrix, $\boldsymbol{\Sigma}$, with the probability density written as

$$\mathcal{N}(\mathbf{x}; \boldsymbol{\mu}, \boldsymbol{\Sigma}) = \frac{1}{(2\pi)^{M/2} \det(\boldsymbol{\Sigma})^{1/2}} \exp\left(\frac{-1}{2}(\mathbf{x} - \boldsymbol{\mu})^\intercal \boldsymbol{\Sigma}^{-1}(\mathbf{x} - \boldsymbol{\mu}) \right). \tag{9}$$

To simplify calculations, we may consider diagonal covariance matrices, $\boldsymbol{\Sigma} = \mathrm{diag}(\boldsymbol{\sigma}^2)$. In particular, the special case where $\boldsymbol{\Sigma} = \mathbf{I}_M$, the $M \times M$ identity matrix, the log-density becomes the *mean squared error*:

$$\log \mathcal{N}(\mathbf{x}; \boldsymbol{\mu}, \mathbf{I}) = -\frac{1}{2}||\mathbf{x} - \boldsymbol{\mu}||_2^2 + \text{const.} \tag{10}$$

Conditional dependencies are mediated by the distribution parameters, which are functions of the conditioning variables. For example, we can express an autoregressive Gaussian distribution (Eq. 2) through $p_\theta(x_j|x_{<j}) = \mathcal{N}(x_j; \mu_\theta(x_{<j}), \sigma_\theta^2(x_{<j}))$, where μ_θ and σ_θ^2 are

functions taking $x_{<j}$ as input. A similar form applies to autoregressive models on sequences of vector inputs (Eq. 3), with $p_\theta(\mathbf{x}_t|\mathbf{x}_{<t}) = \mathcal{N}(\mathbf{x}_t; \boldsymbol{\mu}_\theta(\mathbf{x}_{<t}), \boldsymbol{\Sigma}_\theta(\mathbf{x}_{<t}))$. Likewise, in a latent variable model (Eq. 4), we can express a Gaussian conditional likelihood as $p_\theta(\mathbf{x}|\mathbf{z}) = \mathcal{N}(\mathbf{x}; \boldsymbol{\mu}_\theta(\mathbf{z}), \boldsymbol{\Sigma}_\theta(\mathbf{z}))$. In the above examples, we have used a subscript θ for all functions, however, these may be separate functions in practice.

The functions supplying each of the distribution parameters can range in complexity, from constant to highly non-linear. Classical modeling techniques often employ linear functions. For instance, in a latent variable model, we could parameterize the mean as

$$\boldsymbol{\mu}_\theta(\mathbf{z}) = \mathbf{W}\mathbf{z} + \mathbf{b}, \tag{11}$$

where $\mathbf{W}$ is a matrix of weights and $\mathbf{b}$ is a bias vector. Models of this form underlie factor analysis, probabilistic principal components analysis (Tipping & Bishop, 1999), independent components analysis (Bell & Sejnowski, 1997; Hyvärinen & Oja, 2000), and sparse coding (Olshausen & Field, 1996). While linear models are computationally efficient, they are often too limited to accurately model complex data distributions, e.g., those found in natural images or audio.

Deep learning (Goodfellow et al., 2016) provides probabilistic models with expressive non-linear functions, improving their capacity. In these models, the distribution parameters are parameterized with deep networks, which are then trained by backpropagating (Rumelhart et al., 1986) the gradient of the log-likelihood, $\nabla_\theta \mathbb{E}_{\mathbf{x} \sim \widehat{p}_{\text{data}}} [\log p_\theta(\mathbf{x})]$, through the network. Deep probabilistic models have enabled recent advances in speech (Graves, 2013; van den Oord, Dieleman, et al., 2016), natural language (Sutskever et al., 2014; Radford et al., 2019), images (Razavi et al., 2019), video (Kumar et al., 2020), reinforcement learning (Chua et al., 2018; Ha & Schmidhuber, 2018) and other areas.

In Figure 3, we visualize a computation graph for a deep autoregressive model, breaking the variables into their distributions and terms in the objective. Green circles denote the (Gaussian) conditional likelihoods at each step, which are parameterized by deep networks. The log-likelihood, $\log p_\theta(\mathbf{x}_t|\mathbf{x}_{<t})$, evaluated at the data observation, $\mathbf{x}_t \sim p_{\text{data}}(\mathbf{x}_t|\mathbf{x}_{<t})$ (gray), provides the objective (red dot). The gradient of this objective w.r.t. the network parameters is calculated through backpropagation (red dotted line).

Autoregressive models have proven useful in many domains. However, there are reasons to prefer latent variable models in some contexts. First, autoregressive sampling is inherently sequential, becoming costly in high-dimensional domains. Second, latent variables provide a representation for downstream tasks, compression, and overall data analysis. Finally, latent variables increase flexibility, which is useful for modeling complex distributions with relatively simple, e.g., Gaussian, conditional distributions. While flow-based latent variable models offer one option, their invertibility requirement limits the types of functions that can be used. For these reasons, we require methods for handling the latent marginalization in Eq. 5. Variational inference is one such method.
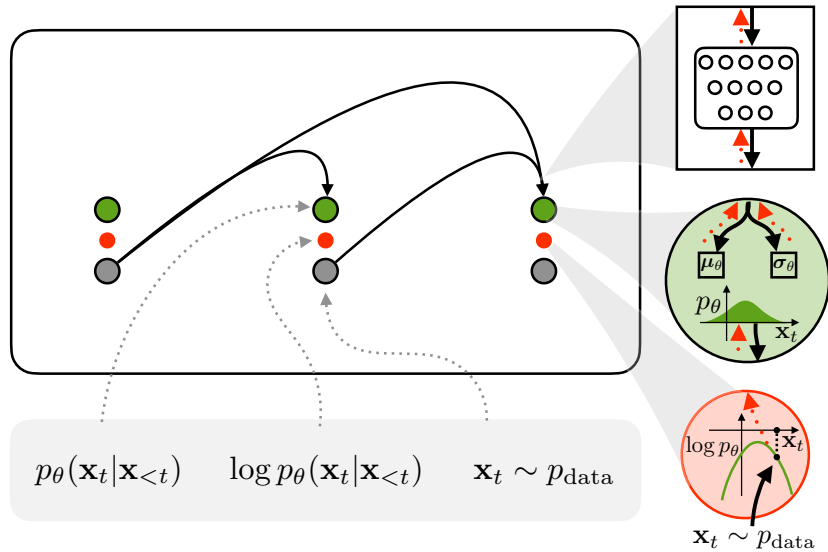
Figure 3: **Autoregressive Computation Graph**. The graph contains the (Gaussian) conditional likelihoods (green), data (gray), and terms in the objective (red dots). Gradients (red dotted lines) backpropagate through the networks parameterizing the distributions.

2.3 Variational Inference

Training latent variable models through maximum likelihood requires evaluating $\log p_\theta(\mathbf{x})$. However, evaluating $p_\theta(\mathbf{x}) = \int p_\theta(\mathbf{x}, \mathbf{z})d\mathbf{z}$ is generally intractable. Thus, we require some technique for approximating $\log p_\theta(\mathbf{x})$. Variational inference (Hinton & Van Camp, 1993; Jordan et al., 1998) approaches this problem by introducing an *approximate posterior* distribution, $q(\mathbf{z}|\mathbf{x})$, which provides a lower bound, $\mathcal{L}(\mathbf{x}; q, \theta) \leq \log p_\theta(\mathbf{x})$. This lower bound is referred to as the evidence (or variational) lower bound (ELBO) as well as the (negative) free energy. By tightening and maximizing the ELBO w.r.t. the model parameters, θ, we can approximate maximum likelihood training.

Variational inference converts probabilistic inference into an optimization problem. Given a family of distributions, $\mathcal{Q}$, e.g., Gaussian, variational inference attempts to find the distribution, $q \in \mathcal{Q}$, that minimizes $D_{\mathrm{KL}}(q(\mathbf{z}|\mathbf{x})||p_\theta(\mathbf{z}|\mathbf{x}))$, where $p_\theta(\mathbf{z}|\mathbf{x})$ is the *posterior* distribution, $p_\theta(\mathbf{z}|\mathbf{x}) = \frac{p_\theta(\mathbf{x}, \mathbf{z})}{p_\theta(\mathbf{x})}$. Because $p_\theta(\mathbf{z}|\mathbf{x})$ includes the intractable $p_\theta(\mathbf{x})$, we cannot minimize this KL divergence directly. Instead, we can rewrite this as

$$D_{\mathrm{KL}}(q(\mathbf{z}|\mathbf{x})||p_\theta(\mathbf{z}|\mathbf{x})) = \log p_\theta(\mathbf{x}) - \mathcal{L}(\mathbf{x}; q, \theta), \tag{12}$$

where, in Eq. 12 (see Appendix A), we have defined $\mathcal{L}(\mathbf{x}; q, \theta)$, as

$$\mathcal{L}(\mathbf{x}; q, \theta) \equiv \mathbb{E}_{\mathbf{z} \sim q(\mathbf{z}|\mathbf{x})} \left[\log p_\theta(\mathbf{x}, \mathbf{z}) - \log q(\mathbf{z}|\mathbf{x}) \right] \tag{13}$$
$$= \mathbb{E}_{\mathbf{z} \sim q(\mathbf{z}|\mathbf{x})} \left[\log p_\theta(\mathbf{x}|\mathbf{z}) \right] - D_{\mathrm{KL}}(q(\mathbf{z}|\mathbf{x})||p_\theta(\mathbf{z})). \tag{14}$$
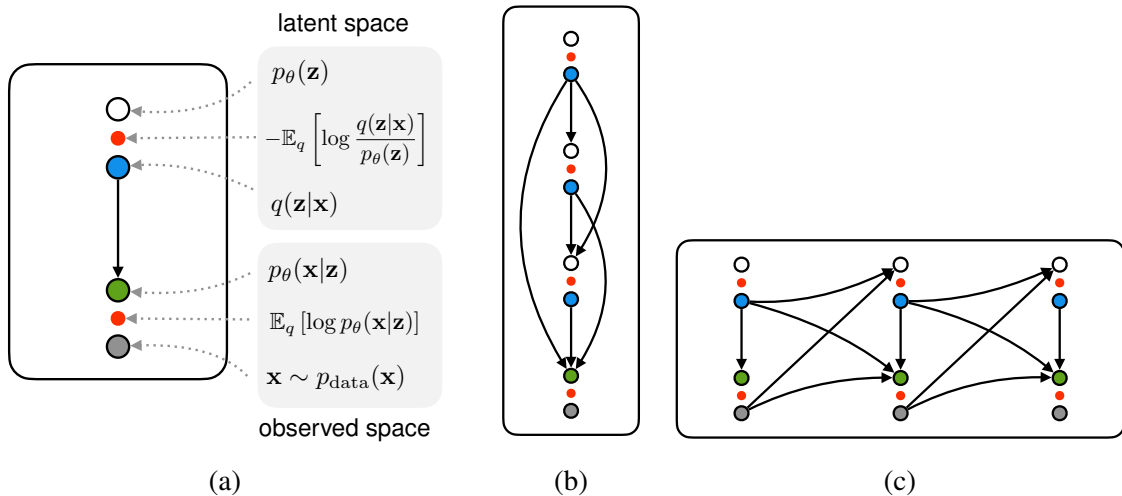
Figure 4: **ELBO Computation Graphs**. **(a)** Basic computation graph for variational inference. Outlined circles denote distributions, smaller red circles denote terms in the ELBO, and arrows denote conditional dependencies. This notation can be used to express **(b)** hierarchical and **(c)** sequential models with various dependencies.

Rearranging terms in Eq. 12, we have

$$\log p_\theta(\mathbf{x}) = \mathcal{L}(\mathbf{x}; q, \theta) + D_{\mathrm{KL}}(q(\mathbf{z}|\mathbf{x})||p_\theta(\mathbf{z}|\mathbf{x})). \tag{15}$$

Because KL divergence is non-negative, $\mathcal{L}(\mathbf{x}; q, \theta) \leq \log p_\theta(\mathbf{x})$, with equality when $q(\mathbf{z}|\mathbf{x}) = p_\theta(\mathbf{z}|\mathbf{x})$. As the LHS of Eq. 15 does not depend on $q(\mathbf{z}|\mathbf{x})$, maximizing $\mathcal{L}(\mathbf{x}; q, \theta)$ w.r.t. q implicitly minimizes $D_{\mathrm{KL}}(q(\mathbf{z}|\mathbf{x})||p_\theta(\mathbf{z}|\mathbf{x}))$ w.r.t. q. Thus, maximizing $\mathcal{L}(\mathbf{x}; q, \theta)$ w.r.t. q tightens the lower bound on $\log p_\theta(\mathbf{x})$. With this tightened lower bound, we can then maximize $\mathcal{L}(\mathbf{x}; q, \theta)$ w.r.t. θ. This alternating optimization process is the variational expectation maximization (EM) algorithm (Dempster et al., 1977; Neal & Hinton, 1998), consisting of approximate inference (E-step) and learning (M-step).

We can also represent the ELBO in latent variable models as a computation graph (Figure 4). Each variable contains a red circle, denoting a term in the ELBO. As compared with the log-likelihood objective, we now have an additional objective term corresponding to the KL divergence for the latent variable. We visualize the variational objective for more complex hierarchical and sequential models in Figures 4b & 4c.

3 Predictive Coding

Predictive coding can be divided into two settings, spatiotemporal and hierarchical, roughly corresponding to the two main forms of probabilistic dependencies. In this section, we review these settings, discussing existing hypothesized correspondences with neural anatomy. We then outline the empirical support for predictive coding, highlighting the need for large-scale, testable models.

3.1 Spatiotemporal Predictive Coding

Spatiotemporal predictive coding (Srinivasan et al., 1982) forms predictions across spatial dimensions and temporal sequences. These predictions produce the resulting "code" as the prediction error. In the temporal setting, we can consider a Gaussian autoregressive model defined over observation sequences, $\mathbf{x}_{1:T}$. The conditional probability at time t is

$$p_\theta(\mathbf{x}_t|\mathbf{x}_{<t}) = \mathcal{N}(\mathbf{x}_t; \boldsymbol{\mu}_\theta(\mathbf{x}_{<t}), \text{diag}(\boldsymbol{\sigma}_\theta^2(\mathbf{x}_{<t}))).$$

Using auxiliary variables, $\mathbf{y}_t \sim \mathcal{N}(\mathbf{0}, \mathbf{I})$, we can express $\mathbf{x}_t = \boldsymbol{\mu}_\theta(\mathbf{x}_{<t}) + \boldsymbol{\sigma}_\theta(\mathbf{x}_{<t}) \odot \mathbf{y}_t$, where $\odot$ denotes element-wise multiplication. Conversely, we can express the inverse, normalization or *whitening* transform as

$$\mathbf{y}_t = \frac{\mathbf{x}_t - \boldsymbol{\mu}_\theta(\mathbf{x}_{<t})}{\boldsymbol{\sigma}_\theta(\mathbf{x}_{<t})}, \tag{16}$$

which is a weighted prediction error.[3] A video example is shown in Figure 5b. The normalization transform removes temporal redundancy in the input, enabling the resulting sequence, $\mathbf{y}_{1:T}$, to be compressed more efficiently (Shannon, 1948; Harrison, 1952; Oliver, 1952). This technique forms the basis of modern video (Wiegand et al., 2003) and audio (Atal & Schroeder, 1979) compression. Note that one special case of this transform is $\boldsymbol{\mu}_\theta(\mathbf{x}_{<t}) = \mathbf{x}_{t-1}$ and $\boldsymbol{\sigma}_\theta(\mathbf{x}_{<t}) = \mathbf{1}$, in which case, $\mathbf{y}_t = \mathbf{x}_t - \mathbf{x}_{t-1} = \Delta\mathbf{x}_t$, i.e., temporal changes. For slowly changing sequences, this is a reasonable choice.

Normalization can also be applied within $\mathbf{x}_t$ to remove spatial dependencies. For instance, we can apply another autoregressive transform over spatial dimensions, predicting the ith dimension, $x_{i,t}$, as a function of previous dimensions, $\mathbf{x}_{1:i,t}$ (Eq. 2). With linear functions, this corresponds to Cholesky whitening (Pourahmadi, 2011; Kingma et al., 2016). However, this imposes an ordering over dimensions. Zero-phase components analysis (ZCA) whitening instead learns symmetric spatial dependencies (Kessy et al., 2018). Modeling these dependencies with a constant covariance matrix, $\boldsymbol{\Sigma}_\theta$, and mean, $\boldsymbol{\mu}_\theta$, the whitening transform is $\mathbf{y} = \boldsymbol{\Sigma}_\theta^{-1/2}(\mathbf{x} - \boldsymbol{\mu}_\theta)$. With natural images, this results in center-surround filters in the rows of $\boldsymbol{\Sigma}_\theta^{-1}$, thereby extracting edges (Figure 5a).

Srinivasan et al. (1982) investigated spatiotemporal predictive coding in the retina, where compression is essential for transmission through the optic nerve. Estimating the (linear) auto-correlation of input sensory signals, they showed that spatiotemporal predictive coding models retinal ganglion cell responses in flies. This scheme allows these neurons to more fully utilize their dynamic range. It is generally accepted that retina, in part, performs stages of spatiotemporal normalization through center-surround receptive fields and on-off responses (Hosoya et al., 2005; Graham et al., 2006; Pitkow & Meister, 2012; Palmer et al., 2015). Dong & Atick (1995) applied similar ideas to thalamus, proposing an additional stage of temporal normalization. This also relates to the notion of generalized coordinates

---

[3]Note that other forms of probabilistic models will result in other forms of whitening transforms.

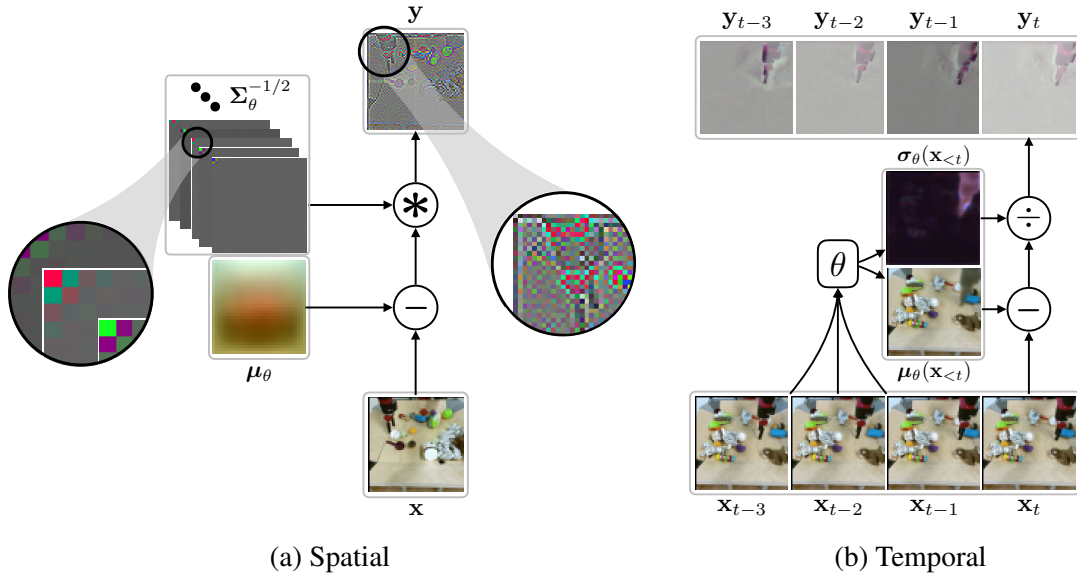|	(a) Spatial	(b) Temporal

Figure 5: **Spatiotemporal Predictive Coding**. **(a)** Spatial predictive coding removes spatial dependencies, using center-surround filters (left) to extract edges (right). **(b)** Temporal predictive coding removes temporal dependencies, extracting motion from video. Video frames are from BAIR Robot Pushing (Ebert et al., 2017).

(Friston, 2008a), i.e., modeling temporal derivatives, which can be approximated using finite differences (prediction errors). That is, $\frac{d\mathbf{x}}{dt} \approx \Delta\mathbf{x}_t \equiv \mathbf{x}_t - \mathbf{x}_{t-1}$. Thus, spatiotemporal predictive coding may be utilized at multiple stages of sensory processing to remove redundancy (Y. Huang & Rao, 2011).

In neural circuits, normalization often involves inhibitory interneurons (Carandini & Heeger, 2012), performing operations similar to those in Eq. 16. For instance, inhibition occurs in retina between photoreceptors, via horizontal cells, and between bipolar cells, via amacrine cells. This can extract unpredicted motion, e.g., an object moving relative to the background (Ölveczky et al., 2003; Baccus et al., 2008). A similar scheme is present in the lateral geniculate nucleus (LGN) in thalamus, with interneurons inhibiting relay cells from retina (Sherman & Guillery, 2002). As mentioned above, this is thought to perform temporal normalization (Dong & Atick, 1995; Dan et al., 1996). Lateral inhibition is also prominent in neocortex, with distinct classes of interneurons shaping the responses of pyramidal neurons (Isaacson & Scanziani, 2011). Part of their computational role appears to be spatiotemporal normalization (Carandini & Heeger, 2012).

3.2   Hierarchical Predictive Coding

Hierarchical predictive coding has been postulated as a model of hierarchical processing in neocortex (Rao & Ballard, 1999; Friston, 2005), the outer sheet-like structure involved in sensory and motor processing (Figure 6). Neocortex is composed of six layers (I–VI),
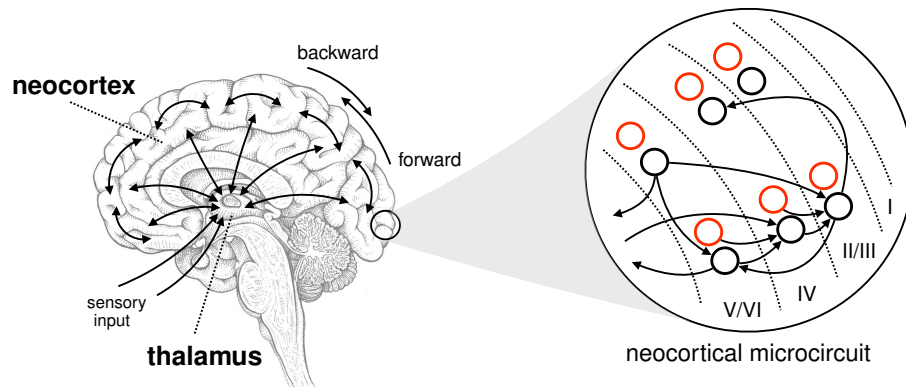
Figure 6: **Brain Anatomy & Cortical Circuitry**. Sensory inputs enter thalamus, forming reciprocal connections with neocortex. Neocortex is composed of six layers, with columns across layers and hierarchies of columns. Black and red circles represent excitatory and inhibitory neurons respectively, with arrows denoting connections. This circuit is repeated with variations throughout neocortex.

with neurons arranged into columns, each engaged in related computations (Mountcastle et al., 1955). Columns interact locally via inhibitory interneurons, while also forming longer-range hierarchies via pyramidal neurons. Such hierarchies characterize multiple perceptual (and motor) processing pathways (Van Essen & Maunsell, 1983). Longer-range connections are split into forward (up the hierarchy) and backward (down) directions. Forward connections are driving, evoking neural activity (Girard & Bullier, 1989; Girard et al., 1991). Backward connections can be modulatory or driving (Covic & Sherman, 2011; De Pasquale & Sherman, 2011), which can be inverted through inhibition (H. S. Meyer et al., 2011). These connections, repeated with variations throughout neocortex, constitute a canonical *neocortical microcircuit* (Douglas et al., 1989), suggesting a single algorithm (Hawkins & Blakeslee, 2004), capable of adapting to various inputs (Sharma et al., 2000).

Formulating a theory of neocortex, Mumford (1992) described thalamus as an 'active blackboard,' with the neocortex attempting to reconstruct the activity in thalamus and lower hierarchical areas. Under this theory, backward projections convey predictions, while forward projections use prediction errors to update estimates. Through a dynamic process, the system settles to an activity pattern, minimizing prediction error. Over time, the parameters are also adjusted to improve predictions. In this way, negative feedback is used, both in inference and learning, to construct a generative model of sensory inputs. Generative state estimation dates back (at least) to Helmholtz (Von Helmholtz, 1867), and error-based updating is inline with cybernetics (Wiener, 1948; MacKay, 1956), which influenced Kalman filtering (Kalman, 1960), a ubiquitous Bayesian filtering algorithm.

A mathematical formulation of Mumford's model, with ties to Kalman filtering (Rao (1998)), was provided by Rao & Ballard (1999), with the generalization to variational inference provided by Friston (2005). To illustrate this setup, consider a model consisting of

13

a single level of continuous latent variables, $\mathbf{z}$, modeling continuous data observations, $\mathbf{x}$. We will use Gaussian densities for each distribution and assume we have

$$p_\theta(\mathbf{x}|\mathbf{z}) = \mathcal{N}(\mathbf{x}; f(\mathbf{W}\mathbf{z}), \mathrm{diag}(\boldsymbol{\sigma}_\mathbf{x}^2)), \tag{17}$$

$$p_\theta(\mathbf{z}) = \mathcal{N}(\mathbf{z}; \boldsymbol{\mu}_\mathbf{z}, \mathrm{diag}(\boldsymbol{\sigma}_\mathbf{z}^2)), \tag{18}$$

where f is an element-wise function (e.g., logistic sigmoid, tanh, or the identity), $\mathbf{W}$ is a weight matrix, $\boldsymbol{\mu}_\mathbf{z}$ is the prior mean, and $\boldsymbol{\sigma}_\mathbf{x}^2$ and $\boldsymbol{\sigma}_\mathbf{z}^2$ are vectors of variances.

In the simplest approach to inference, we can find the maximum-a-posteriori (MAP) estimate, i.e., estimate the $\mathbf{z}^*$ which maximizes $p_\theta(\mathbf{z}|\mathbf{x})$. While we cannot tractably evaluate $p_\theta(\mathbf{z}|\mathbf{x}) = \frac{p_\theta(\mathbf{x},\mathbf{z})}{p_\theta(\mathbf{x})}$ directly, we can write

$$\begin{aligned} \mathbf{z}^* &= \arg\max_\mathbf{z} \frac{p_\theta(\mathbf{x}, \mathbf{z})}{p_\theta(\mathbf{x})} \\ &= \arg\max_\mathbf{z} p_\theta(\mathbf{x}, \mathbf{z}). \end{aligned}$$

Thus, we can perform inference using the joint distribution, $p_\theta(\mathbf{x}, \mathbf{z}) = p_\theta(\mathbf{x}|\mathbf{z})p_\theta(\mathbf{z})$, which we can tractably evaluate. We can also replace the optimization over the probability distribution with an optimization over the $\log$ probability, since $\log(\cdot)$ is a monotonically increasing function and does not affect the optimization. We then have

$$\begin{aligned} \mathbf{z}^* &= \arg\max_\mathbf{z} \left[\log p_\theta(\mathbf{x}|\mathbf{z}) + \log p_\theta(\mathbf{z}) \right]. \\ &= \arg\max_\mathbf{z} \left[\log \mathcal{N}(\mathbf{x}; f(\mathbf{W}\mathbf{z}), \mathrm{diag}(\boldsymbol{\sigma}_\mathbf{x}^2)) + \log \mathcal{N}(\mathbf{z}; \boldsymbol{\mu}_\mathbf{z}, \mathrm{diag}(\boldsymbol{\sigma}_\mathbf{z}^2)) \right]. \end{aligned}$$

Each of the terms in this objective is a weighted squared error. For instance, the first term is the weighted squared error in reconstructing the data observation:

$$\log \mathcal{N}(\mathbf{x}; f(\mathbf{W}\mathbf{z}), \mathrm{diag}(\boldsymbol{\sigma}_\mathbf{x}^2)) = \frac{-M}{2} \log(2\pi) - \frac{1}{2} \log \det \left(\mathrm{diag}(\boldsymbol{\sigma}_\mathbf{x}^2) \right) - \frac{1}{2} \left\| \frac{\mathbf{x} - f(\mathbf{W}\mathbf{z})}{\boldsymbol{\sigma}_\mathbf{x}} \right\|_2^2,$$

where M is the dimensionality of $\mathbf{x}$ and $|| \cdot ||_2^2$ denotes the squared L2 norm. Plugging these terms into the objective and dropping terms that do not depend on $\mathbf{z}$ yields

$$\mathbf{z}^* = \arg\max_\mathbf{z} \underbrace{\left[\frac{-1}{2} \left\| \frac{\mathbf{x} - f(\mathbf{W}\mathbf{z})}{\boldsymbol{\sigma}_\mathbf{x}} \right\|_2^2 - \frac{1}{2} \left\| \frac{\mathbf{z} - \boldsymbol{\mu}_\mathbf{z}}{\boldsymbol{\sigma}_\mathbf{z}} \right\|_2^2 \right]}_{\mathscr{L}(\mathbf{z}; \theta)}, \tag{19}$$

where we have defined the objective as $\mathscr{L}(\mathbf{z}; \theta)$. For purposes of illustration, let us assume that $f(\cdot)$ is the identity function, i.e., $f(\mathbf{W}\mathbf{z}) = \mathbf{W}\mathbf{z}$. We can then evaluate the gradient of $\mathscr{L}(\mathbf{z}; \theta)$ w.r.t. $\mathbf{z}$, yielding

$$\nabla_\mathbf{z} \mathscr{L}(\mathbf{z}; \theta) = \mathbf{W}^\mathsf{T} \underbrace{\left(\frac{\mathbf{x} - \mathbf{W}\mathbf{z}}{\boldsymbol{\sigma}_\mathbf{x}} \right)}_{\xi_\mathbf{x}} - \underbrace{\frac{\mathbf{z} - \boldsymbol{\mu}_\mathbf{z}}{\boldsymbol{\sigma}_\mathbf{z}}}_{\xi_\mathbf{z}}. \tag{20}$$
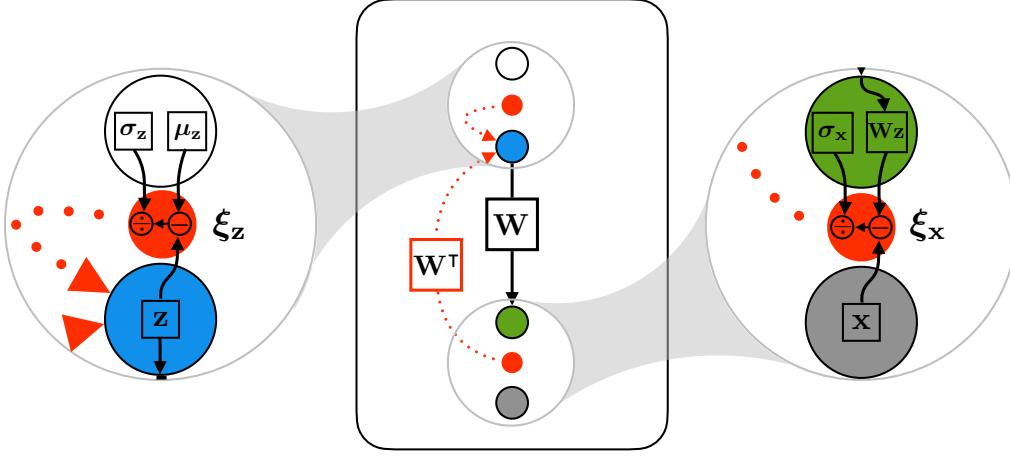
Figure 7: **Hierarchical Predictive Coding**. The diagram shows the basic computation graph for a Gaussian latent variable model with MAP inference. The insets show the weighted error calculation for the latent (left) and observed (right) variables.

The transposed weight matrix, $\mathbf{W}^{\intercal}$, results from differentiating $\mathbf{W}\mathbf{z}$, translating the reconstruction error into an update in $\mathbf{z}$. We have also defined the weighted errors, $\boldsymbol{\xi}_{\mathbf{x}}$ and $\boldsymbol{\xi}_{\mathbf{z}}$. From Eq. 20, we see that if we want to perform inference using gradient-based optimization, e.g., $\mathbf{z} \leftarrow \mathbf{z} + \alpha \nabla_{\mathbf{z}} \mathcal{L}(\mathbf{z}; \theta)$, we need 1) the weighted errors, $\boldsymbol{\xi}_{\mathbf{x}}$ and $\boldsymbol{\xi}_{\mathbf{z}}$, and 2) the transposed weights, $\mathbf{W}^{\intercal}$, or more generally, the Jacobian of the conditional likelihood mean. This overall scheme is depicted in Figure 7.

To learn the weight parameters, we can differentiate $\mathcal{L}(\mathbf{z}; \theta)$ (Eq. 19) w.r.t. $\mathbf{W}$:

$$\nabla_{\mathbf{W}} \mathcal{L}(\mathbf{z}; \theta) = \boldsymbol{\xi}_{\mathbf{x}} \mathbf{z}^{\intercal}.$$

This gradient is the product of a local error, $\boldsymbol{\xi}_{\mathbf{x}}$, and the latent variable, $\mathbf{z}$, suggesting the possibility of a biologically-plausible learning rule (Whittington & Bogacz, 2017).

Predictive coding identifies the conditional likelihood (Eq. 17) with backward (top-down) cortical projections, whereas inference (Eq. 20) is identified with forward (bottom-up) projections (Friston, 2005). Each are thought to be mediated by pyramidal neurons. Under this model, each cortical column predicts and estimates a stochastic continuous latent variable, possibly represented via a (pyramidal) firing rate or membrane potential (Friston, 2005). Interneurons within columns calculate errors ($\boldsymbol{\xi}_{\mathbf{x}}$ and $\boldsymbol{\xi}_{\mathbf{z}}$). Although we have only discussed diagonal covariance ($\boldsymbol{\sigma}_{\mathbf{x}}^2$ and $\boldsymbol{\sigma}_{\mathbf{z}}^2$), lateral inhibitory interneurons could parameterize full covariance matrices, i.e., $\boldsymbol{\Sigma}_{\mathbf{x}}$ and $\boldsymbol{\Sigma}_{\mathbf{z}}$, as a form of *spatial* predictive coding (Section 3.1). These factors weight $\boldsymbol{\xi}_{\mathbf{x}}$ and $\boldsymbol{\xi}_{\mathbf{z}}$, modulating the *gain* of each error as a form of "attention" (Feldman & Friston, 2010). Neural correspondences are summarized in Table 1.

We have presented a simplified model of hierarchical predictive coding, without multiple latent levels and dynamics. A full hierarchical predictive coding model would include these

Table 1: **Neural Correspondences of Hierarchical Predictive Coding**.

Neuroscience	Predictive Coding
Top-Down Cortical Projections	Generative Model Conditional Mapping
Bottom-Up Cortical Projections	Inference Updating
Lateral Inhibition	Covariance Matrices
(Pyramidal) Neuron Activity	Latent Variable Estimates & Errors
Cortical Column	Corresponding Estimate & Error

aspects and others. In particular, Friston has explored various design choices (Friston et al., 2007; Friston, 2008a,b), yet the core aspects of probabilistic generative modeling and variational inference remain the same. Elaborating and comparing these choices will be essential for empirically validating hierarchical predictive coding.

3.3   Empirical Support

While there is considerable evidence in support of predictions and errors in neural systems, disentangling these general aspects of predictive coding from the particular algorithmic choices remains challenging (Gershman, 2019). Here, we outline relevant work, but we refer to Y. Huang & Rao (2011); Bastos et al. (2012); Clark (2013); Keller & Mrsic-Flogel (2018); Walsh et al. (2020) for a more in-depth overview.

Spatiotemporal   Various works have investigated predictive coding in early sensory areas, e.g., retina (Srinivasan et al., 1982; Atick & Redlich, 1992). This involves fitting retinal ganglion cell responses to a spatial whitening (or decorrelation) process (Graham et al., 2006; Pitkow & Meister, 2012), which can be dynamically adjusted (Hosoya et al., 2005). Similar analyses suggest that retina also employs temporal predictive coding (Srinivasan et al., 1982; Palmer et al., 2015). Such models typically contain linear whitening filters (center-surround) followed by non-linearities. These non-linearities have been shown to be essential for modeling responses (Pitkow & Meister, 2012), possibly by inducing added sparsity (Graham et al., 2006). Spatiotemporal predictive coding also appears to be found in thalamus (Dong & Atick, 1995; Dan et al., 1996) and cortex, however, such analyses are complicated by backward, modulatory inputs.

Hierarchical   Early work toward empirically validating hierarchical predictive coding came from explaining extra-classical receptive field effects (Rao & Ballard, 1999; Rao & Sejnowski, 2002), whereby top-down signals in cortex alter classical visual receptive fields, suggesting that top-down influences play a key role in sensory processing (Gilbert & Sigman, 2007). Note that such effects support a cortical generative model generally (Olshausen & Field, 1997), not predictive coding specifically.

Temporal influences have been demonstrated through repetition suppression (Summerfield et al., 2006), in which activity diminishes in response to repeated, i.e., predictable, stimuli. This may reflect error suppression from improved predictions. Predictive coding has also been used to explain biphasic responses in LGN (Jehee & Ballard, 2009), in which reversing the visual input with an anti-correlated image results in a large response, presumably due to prediction errors. Predictive signals have been documented in auditory (Wacongne et al., 2011) and visual (T. Meyer & Olson, 2011) processing. Activity seemingly corresponding to prediction errors has also been observed in a variety of areas and contexts, including visual cortex in mice (Keller et al., 2012; Zmarz & Keller, 2016; Gillon et al., 2021), auditory cortex in monkeys (Eliades & Wang, 2008) and rodents (Parras et al., 2017), and visual cortex in humans (Murray et al., 2002; Alink et al., 2010; Egner et al., 2010). Thus, sensory cortex appears to be engaged in hierarchical and temporal prediction, with prediction errors playing a key role.

Empirical evidence for predictive coding aside, given the complexity of neural systems, the theory is undoubtedly incomplete or incorrect. Without the low-level details, e.g., connectivity, potentials, etc., it is difficult to determine the computational form of the circuit. Further, these models are typically oversimplified, with few trained parameters, detached from natural stimuli. While new tools enable us to test predictive coding in neural circuits (Gillon et al., 2021), machine learning, particularly VAEs, can advance from the other direction. Training large-scale models on natural stimuli may improve empirical predictions for biological systems (Rao & Ballard, 1999; Lotter et al., 2018).

4 Variational Autoencoders

Variational autoencoders (VAEs) (Kingma & Welling, 2014; Rezende et al., 2014) are latent variable models parameterized by deep networks. As in hierarchical predictive coding, these models typically contain Gaussian latent variables and are trained using variational inference. However, rather than performing inference optimization directly, VAEs *amortize* inference (Gershman & Goodman, 2014).

4.1 Amortized Variational Inference

Amortization refers to spreading out costs. In amortized inference, these are the computational costs of inference. With $q(\mathbf{z}|\mathbf{x}) = \mathcal{N}(\mathbf{z}; \boldsymbol{\mu}_q, \mathrm{diag}(\boldsymbol{\sigma}_q^2))$ and $\boldsymbol{\lambda} \equiv [\boldsymbol{\mu}_q, \boldsymbol{\sigma}_q]$, rather than separately optimizing $\boldsymbol{\lambda}$ for each data example, we amortize this optimization using a learned optimizer or *inference model*. By using meta-optimization, we can perform inference optimization far more efficiently. Inference models are linked with deep latent variable models, popularized by the Helmholtz Machine (Dayan et al., 1995), a form of *autoencoder* (Ballard, 1987). Here, the inference model is a direct mapping from $\mathbf{x}$ to $\boldsymbol{\lambda}$:

$$\boldsymbol{\lambda} \leftarrow f_\phi(\mathbf{x}), \tag{21}$$
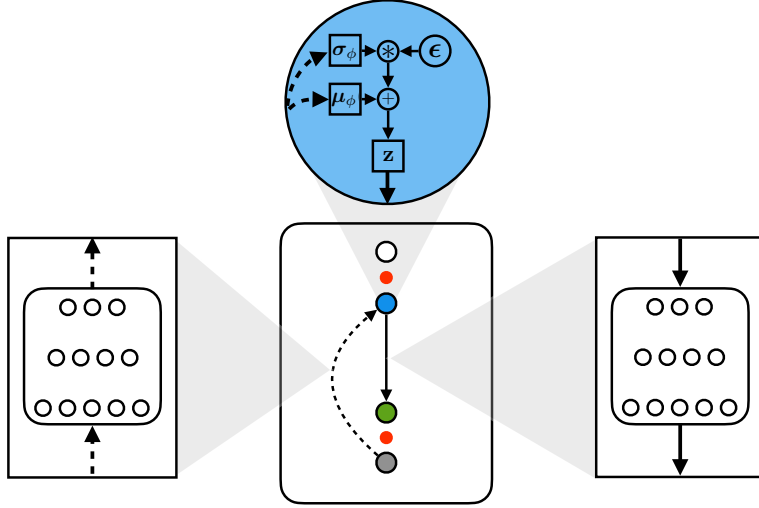
Figure 8: **Variational Autoencoder**. VAEs use direct amortization (Eq. 21) to train deep latent variable models. The inference model (left) is an *encoder*, and the conditional likelihood (right) is a *decoder*. Each are parameterized by deep networks.

where f_ϕ is a function (deep network) with parameters ϕ. We then denote the approximate posterior as $q_\phi(\mathbf{z}|\mathbf{x})$ to denote the parameterization by ϕ. Now, rather than optimizing $\boldsymbol{\lambda}$ using gradient-based techniques, we update ϕ using $\nabla_\phi \mathcal{L} = \frac{\partial \mathcal{L}}{\partial \boldsymbol{\lambda}} \frac{\partial \boldsymbol{\lambda}}{\partial \phi}$, thereby letting f_ϕ learn to optimize $\boldsymbol{\lambda}$. This procedure is simple, as we only need to tune the learning rate for ϕ, and efficient, as we have an estimate of $\boldsymbol{\lambda}$ after one forward pass through f_ϕ. Amortization is also widely applicable: if we can estimate $\nabla_{\boldsymbol{\lambda}} \mathcal{L}$, we can continue differentiating through the chain $\phi \to \boldsymbol{\lambda} \to \mathbf{z} \to \mathcal{L}$.

To differentiate through $\mathbf{z} \sim q_\phi(\mathbf{z}|\mathbf{x})$, we can use the pathwise derivative estimator, also referred to as the reparameterization estimator (Kingma & Welling, 2014). This is accomplished by expressing $\mathbf{z}$ in terms of an auxiliary random variable. The most common example expresses $\mathbf{z} \sim \mathcal{N}(\mathbf{z}; \boldsymbol{\mu}_q, \text{diag}(\boldsymbol{\sigma}_q^2))$ as $\mathbf{z} = \boldsymbol{\mu}_q + \boldsymbol{\epsilon} \odot \boldsymbol{\sigma}_q$, where $\boldsymbol{\epsilon} \sim \mathcal{N}(\boldsymbol{\epsilon}; \mathbf{0}, \mathbf{I})$ and $\odot$ denotes element-wise multiplication. We can then estimate $\nabla_{\boldsymbol{\mu}_q} \mathcal{L}$ and $\nabla_{\boldsymbol{\sigma}_q} \mathcal{L}$, allowing us to calculate the inference model gradients, $\nabla_\phi \mathcal{L}$.

When direct amortization is combined with the pathwise derivative estimator in deep latent variable models, the resulting setup is a *variational autoencoder* (Kingma & Welling, 2014; Rezende et al., 2014). In this interpretation, $q_\phi(\mathbf{z}|\mathbf{x})$ is an *encoder*, $\mathbf{z}$ is the latent *code*, and $p_\theta(\mathbf{x}|\mathbf{z})$ is a *decoder* (Figure 8). This direct encoding scheme is intuitive: in the same way that $p_\theta(\mathbf{x}|\mathbf{z})$ directly maps $\mathbf{z}$ to a distribution over $\mathbf{x}$, $q_\phi(\mathbf{z}|\mathbf{x})$ directly maps $\mathbf{x}$ to a distribution over $\mathbf{z}$. Indeed, with perfect knowledge of $p_\theta(\mathbf{x}, \mathbf{z})$, f_ϕ could act as a lookup table, mapping each $\mathbf{x}$ to the corresponding optimal $\boldsymbol{\lambda}$. However, in practice, direct amortization of this form tends to result in suboptimal estimates of $\boldsymbol{\lambda}$ (Cremer et al., 2018), motivating more powerful amortized inference techniques.

4.1.1 Iterative Amortized Inference

One method for improving direct amortization involves incorporating iterative updates (Hjelm et al., 2016; Krishnan et al., 2018; Kim et al., 2018; Marino, Yue, & Mandt, 2018), replacing a one-step inference procedure with a multi-step procedure. Iterative amortized inference (Marino, Yue, & Mandt, 2018) maintains an inference model, but uses it to perform iterative updates on the approximate posterior. Following the previous notation, the basic form of an iterative amortized inference model is given as:

$$\boldsymbol{\lambda} \leftarrow f_\phi(\boldsymbol{\lambda}, \nabla_{\boldsymbol{\lambda}} \mathcal{L}). \tag{22}$$

Iterative inference models take in the current estimate, $\boldsymbol{\lambda}$, as well as the gradient, $\nabla_{\boldsymbol{\lambda}} \mathcal{L}$, and output an updated estimate of $\boldsymbol{\lambda}$. As before, inference model parameters are updated using estimates of $\nabla_\phi \mathcal{L}$. Note that Eq. 22 generalizes stochastic gradient-based optimization. For instance, a special case is $\boldsymbol{\lambda} \leftarrow \boldsymbol{\lambda} + \alpha \nabla_{\boldsymbol{\lambda}} \mathcal{L}$, where α is a step-size, however, Eq. 22 also includes non-linear updates (Andrychowicz et al., 2016).

In latent Gaussian models, $\nabla_{\boldsymbol{\lambda}}$ is defined by the weighted errors, $\boldsymbol{\xi}_{\mathbf{x}}$ and $\boldsymbol{\xi}_{\mathbf{z}}$, and the Jacobian of the conditional likelihood, $\mathbf{J}$ ($\mathbf{W}$ in the linear model in Section 3.2). Thus, in latent Gaussian models, we can consider inference models of the special form:

$$\boldsymbol{\lambda} \leftarrow f_\phi(\boldsymbol{\lambda}, \boldsymbol{\xi}_{\mathbf{x}}, \boldsymbol{\xi}_{\mathbf{z}}). \tag{23}$$

This is a learned, non-linear mapping from errors to updated estimates of the approximate posterior, i.e., learned negative feedback. The distinction between direct and iterative amortization is shown in Figures 10b & 10c. Iterative amortization can be readily extended to sequential models (Marino, Cvitkovic, & Yue, 2018), resulting in a general predict-update inference scheme, highly reminiscent of Kalman filtering (Kalman, 1960).

4.2 Extensions of VAEs

4.2.1 Additional Dependencies & Representation Learning

VAEs have been extended to a variety of architectures, incorporating hierarchical and temporal dependencies. Sønderby et al. (2016) proposed a hierarchical VAE, in which the conditional prior at each level, ℓ, i.e., $p_\theta(\mathbf{z}^\ell | \mathbf{z}^{\ell+1:L})$, is parameterized by a deep network (see Eq. 7). Follow-up works have scaled this approach with impressive results (Kingma et al., 2016; Vahdat & Kautz, 2020; Child, 2020), extracting increasingly abstract features at higher levels (Maaløe et al., 2019). Another line of work has incorporated temporal dependencies within VAEs, parameterizing dynamics in the prior and conditional likelihood with deep networks (Chung et al., 2015; Fraccaro et al., 2016). Such models can also provide representations and predictions for reinforcement learning (Ha & Schmidhuber, 2018; Hafner et al., 2019).

Other works have investigated representation learning within VAEs. One approach, the β-VAE (Higgins et al., 2017), modifies the ELBO (Eq. 14) by adjusting a weighting,
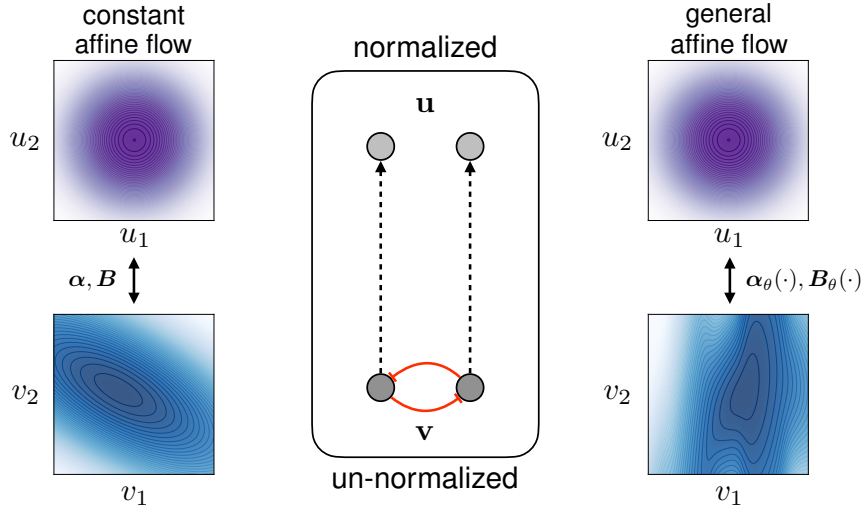
Figure 9: **Normalizing Flows**. Normalizing flows is a framework for adding or removing dependencies. Using affine parameter functions, $\boldsymbol{\alpha}_\theta$ and $\boldsymbol{B}_\theta$, one can model non-linear dependencies, generalizing constant transforms, e.g., a covariance matrix.

β, on $D_{\mathrm{KL}}(q(\mathbf{z}|\mathbf{x})||p_\theta(\mathbf{z}))$. This tends to yield more disentangled, i.e., independent, latent variables. Indeed, β controls the rate-distortion trade-off between latent complexity and reconstruction (Alemi et al., 2018), highlighting VAEs' ability to extract latent structure at multiple resolutions (Rezende & Viola, 2018). Likewise, a separate line of work has focused on identifiability, i.e., the ability to uniquely recover the original latent variables within a model (or their posterior). While this is true in linear ICA (Comon, 1994), it is not generally the case with non-linear ICA and non-invertible models (VAEs) (Khemakhem et al., 2020; Gresele et al., 2020), requiring special considerations.

4.2.2 Normalizing Flows

Another direction within VAEs is the use of normalizing flows (Rezende & Mohamed, 2015). Flow-based distributions use invertible transforms to add and remove dependencies (Section 2.2.1). While such models can operate as generative models (Dinh et al., 2015, 2017; Papamakarios et al., 2017), they can also define distributions in VAEs. This includes the approximate posterior (Rezende & Mohamed, 2015), prior (C.-W. Huang et al., 2017), and conditional likelihood (Agrawal & Dukkipati, 2016). In each case, a deep network outputs the parameters (e.g., mean and variance) of a *base distribution* over a normalized variable. Separate deep networks parameterize the transforms, which map between the normalized and unnormalized variables.

Example: Consider a normalized variable, $\mathbf{u}$, defined by the distribution $p_\theta(\mathbf{u}|\cdot) = \mathcal{N}(\mathbf{u}; \boldsymbol{\mu}_\theta(\cdot), \mathrm{diag}(\boldsymbol{\sigma}_\theta^2(\cdot)))$, where $\boldsymbol{\mu}_\theta$ and $\boldsymbol{\sigma}_\theta$ are output by deep networks, with $\cdot$ denoting conditioning input variables. We consider an *affine* transform (Dinh et al., 2017), defined

by a shift vector, $\boldsymbol{\alpha} = \boldsymbol{\alpha}_\theta(\mathbf{u})$, and a scale matrix, $\boldsymbol{B} = \boldsymbol{B}_\theta(\mathbf{u})$, each of which may be parameterized by deep networks. This defines a new, un-normalized variable $\mathbf{v}$:

$$\mathbf{v} = \boldsymbol{\alpha} + \boldsymbol{B}\mathbf{u}, \tag{24}$$

which can now contain affine dependencies between dimensions. For Eq. 24 to be invertible, we require that $\boldsymbol{B}$ itself is invertible, i.e., non-zero determinant. Thus, $\boldsymbol{B}$ is a square matrix, and $\mathbf{u}$ and $\mathbf{v}$ are the same dimensionality. If, instead, we are given $\mathbf{v}$, we can calculate its log-probability by applying the normalizing inverse transform to get $\mathbf{u}$:

$$\mathbf{u} = \boldsymbol{B}^{-1}(\mathbf{v} - \boldsymbol{\alpha}), \tag{25}$$

then use the change of variables formula (Eq. 6). This converts the log-probability calculation from the structured space of $\mathbf{v}$ to the normalized space of $\mathbf{u}$. Note that the multivariate Gaussian density (Eq. 9) is a special case of this transform, taking a standard Gaussian variable, $\mathbf{u} \sim \mathcal{N}(\mathbf{u}; \mathbf{0}, \mathbf{I})$, and adding linear dependencies to yield a multivariate Gaussian variable, $\mathbf{v} \sim \mathcal{N}(\mathbf{v}; \boldsymbol{\alpha}, \boldsymbol{B}^\intercal \boldsymbol{B})$. In this case, where $\boldsymbol{\alpha}$ and $\boldsymbol{B}$ are constant, the inverse transform removes linear dependencies between dimensions in $\mathbf{v}$. We depict this scheme in Figure 9, along with the more general non-linear version provided by normalizing flows, in which $\boldsymbol{\alpha}_\theta$ and $\boldsymbol{B}_\theta$ are functions. Thus, normalizing flows provides a powerful, more general approach for augmenting the distributions in latent variable models, applicable both across space (Rezende & Mohamed, 2015; Kingma et al., 2016) and time (van den Oord et al., 2018; Marino et al., 2020).

5 Connections & Comparisons

Predictive coding and VAEs (and deep generative models generally), are highly related, both in their model formulations and inference approaches (Figure 10). Specifically,

- **Model Formulation**: Both areas consider hierarchical latent Gaussian models with non-linear dependencies between latent levels, as well as dependencies within levels via covariance matrices (predictive coding) or normalizing flows (VAEs).

- **Inference**: Both areas use variational inference, often with Gaussian approximate posteriors. While predictive coding and VAEs employ differing optimization techniques, these are design choices in solving the same inference problem.

These similarities reflect a common mathematical foundation inherited from cybernetics and descendant fields. We now discuss these two points in more detail.

5.1 Model Formulation

The primary distinction in model formulation is the form of the (non-linear) functions parameterizing dependencies. Rao & Ballard (1999) parameterize the conditional likelihood

as a linear function followed by an element-wise non-linearity. Friston has considered a wider range of functions, e.g., polynomial (Friston, 2008a), however, such functions are rarely learned. VAEs instead parameterize these functions using deep networks with multiple layers. The deep network weights are trained through backpropagation, enabling the wide application of VAEs to various data domains.

Predictive coding and VAEs also consider dependencies within each level. Friston (2005) uses full-covariance Gaussian densities, with the inverse of the covariance matrix (precision) parameterizing linear dependencies within a level. Rao & Ballard (1999) normalize the observations, modeling linear dependencies within the conditional likelihood. These are linear special cases of the more general technique of normalizing flows (Rezende & Mohamed, 2015): a covariance matrix is an affine normalizing flow with linear dependencies (Kingma et al., 2016). Normalizing flows have been applied throughout each of the distributions within VAEs (Section 4.2.2), modeling non-linear dependencies across both spatial and temporal dimensions. These flows are also parameterized by deep networks, providing a flexible, yet general modeling approach.

Related to normalization, there are proposals within predictive coding that the precision of the prior could mediate a form of attention (Feldman & Friston, 2010). Increasing the precision of a variable serves as a form of gain modulation, up-weighting the error in the objective function, thereby enforcing more accurate inference estimates. This concept is absent from VAEs. However, as VAEs become more prevalent in interactive settings (Ha & Schmidhuber, 2018), i.e., beyond pure generative modeling, this may become crucial in steering models toward task-relevant perceptual inferences.

Finally, predictive coding and VAEs have both been extended to sequential settings. In predictive coding, sequential dependencies may be parameterized by linear functions (Srinivasan et al., 1982) or so-called generalized coordinates (Friston, 2008a), modeling multiple orders of motion. In extensions of VAEs, sequential dependencies are again parameterized by deep networks, in many cases using recurrent networks (Chung et al., 2015; Fraccaro et al., 2016). Thus, while the specific implementations vary, in either case, sequential dependencies are ultimately functions, which are subject to design choices.

5.2 Inference

Although both predictive coding and VAEs typically use variational inference with Gaussian approximate posteriors, Sections 3 & 4 illustrate key differences (Figure 10). Predictive coding generally relies on *gradient-based* optimization to perform inference, whereas VAEs employ *amortized* optimization. While these approaches may, at first, appear radically different, hybrid error-encoding inference approaches (Eq. 23), such as PredNet (Lotter et al., 2017) and iterative amortization (Marino, Yue, & Mandt, 2018), provide a link. Such approaches receive errors as input, as in predictive coding, however, they have learnable parameters, i.e., amortization. In fact, amortization may provide a crucial element for implementing predictive coding in biological neural networks.

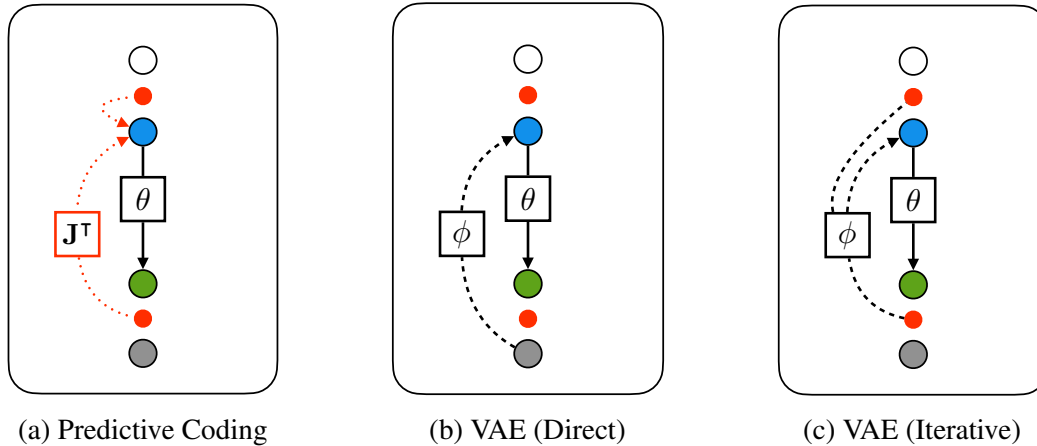Though rarely discussed, hierarchical predictive coding assumes that the inference

Figure 10: **Hierarchical Predictive Coding & VAEs**. Computation diagrams for **(a)** hierarchical predictive coding, **(b)** VAE with direct amortized inference, and **(c)** VAE with iterative amortized inference (Marino, Yue, & Mandt, 2018). $\mathbf{J}^\top$ denotes the transposed Jacobian matrix of the conditional likelihood. Red dotted lines denote gradients, and black dashed lines denote amortized inference.

gradients, supplied by forward connections, can be readily calculated. But, as seen in Section 3.2, the weights of these forward connections are the transposed Jacobian matrix of the backward connections (Rao & Ballard, 1999). This is an example of the *weight transport* problem (Grossberg, 1987), in which the weights of one set of connections (forward) depend on the weights of another set of connections (backward). This is generally regarded as not being biologically-plausible.

Amortization provides a solution to this problem: *learn* to perform inference. Rather than transporting the generative weights to the inference connections, amortization learns a separate set of inference weights, potentially using local learning rules (Bengio, 2014; Lee et al., 2015). Thus, despite criticism from Friston (2018), amortization may offer a more biologically-plausible inference approach. Further, amortized inference yields accurate estimates with exceedingly few iterations: even a single iteration may yield reasonable estimates (Marino, Yue, & Mandt, 2018). These computational efficiency benefits provide another argument in favor of amortization.

Finally, although predictive coding and VAEs typically assume Gaussian approximate posteriors, there is one additional difference in the ways in which these parameters are conventionally calculated. Friston often uses the Laplace approximation[4] (Friston et al., 2007), solving directly for the optimal Gaussian variance, whereas VAEs treat this as another output of the inference model (Kingma & Welling, 2014; Rezende et al., 2014). These approaches can be applied in either setting, e.g., Park et al. (2019).

---

[4]This is not to be confused with a Laplace distribution. The approximate posterior is still Gaussian.
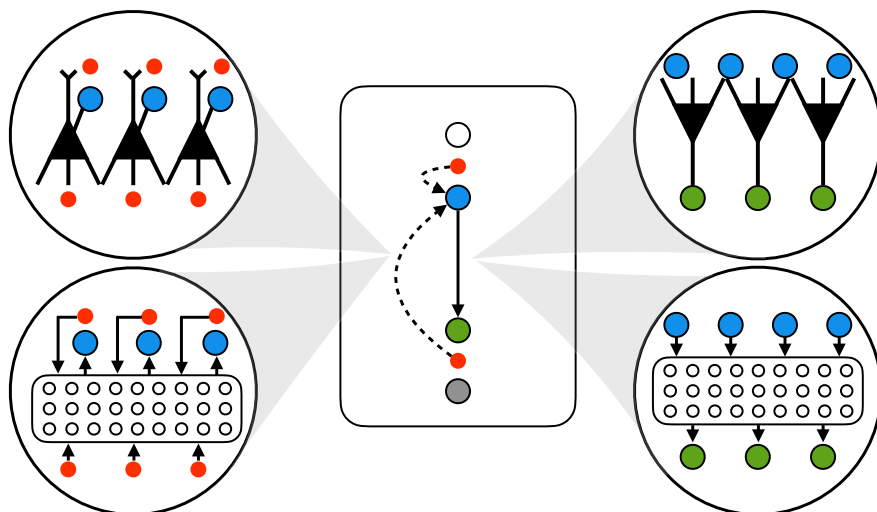
Figure 11: **Pyramidal Neurons & Deep Networks**. Connecting VAEs with predictive coding places deep networks (*bottom*) in correspondence with the dendrites of pyramidal neurons (*top*), both for generation (*right*) and (amortized) inference (*left*).

6 Correspondences

Having connected VAEs and predictive coding, we now discuss possible correspondences between machine learning and neuroscience. In Table 1, top-down and bottom-up cortical projections, each mediated by pyramidal neurons, respectively parameterize the generative model and inference updates. Mapping this onto VAEs suggests that **deep (artificial) neural networks are in correspondence with pyramidal neuron dendrites** (Figure 11, Right), or, more specifically, a deep network corresponds to a collection of pyramidal dendrites operating in parallel. Predictive coding also postulates that lateral interneurons parameterize dependencies within variables as inverse covariance matrices. VAEs parameterize these dependencies using more general normalizing flows, suggesting that **normalizing flows are in correspondence with lateral interneurons**. While normalizing flows also use deep networks, the effect that they have on computation tends to be restricted and simple (e.g., affine). We now briefly discuss these correspondences.

6.1 Pyramidal Neurons & Deep Networks

Non-linear Dendritic Computation   Placing deep networks in correspondence with pyramidal dendrites suggests that (some) biological neurons may be better computationally described as *non-linear* functions. Evidence from neuroscience supports this claim. Early simulations showed that individual pyramidal neurons, through dendritic processing, could operate as multi-layer artificial networks (Zador et al., 1992; Mel, 1992). This was later supported by empirical findings that pyramidal dendrites act as computational 'subunits,'
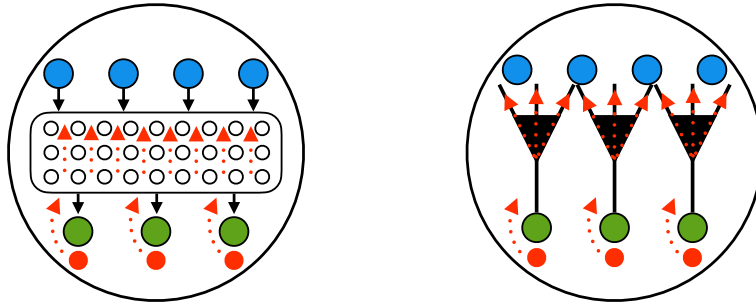
Figure 12: **Backpropagation Within Neurons**. If deep networks are in correspondence with pyramidal neurons, this implies that backpropagation (*left*) is analogous to learning within neurons, perhaps via backpropagating action potentials (*right*).

yielding the equivalent of a two-layer artificial network (Poirazi et al., 2003; Polsky et al., 2004). More recently, Gidon et al. (2020) demonstrated that individual pyramidal neurons can compute the XOR operation, which requires non-linear processing. This is supported by further modeling work (Jones & Kording, 2020; Beniaguev et al., 2021). Positing a more substantial role for dendritic computation (London & Häusser, 2005) moves beyond the simplistic comparison of biological and artificial neurons that currently dominates. Instead, neural computation depends on morphology and circuits.

Amortization   Pyramidal neurons mediate both top-down and bottom-up cortical projections. Under predictive coding, this suggests that inference relies on learned, non-linear functions, i.e., *amortization*. One such implementation is through pyramidal neurons with separate apical and basal dendrites, which, respectively, receive top-down and bottom-up inputs (Bekkers, 2011; Guergiuev et al., 2016). Recent evidence from Gillon et al. (2021) suggests that these are top-down predictions and bottom-up errors. These neurons may implement iterative amortized inference (Marino, Yue, & Mandt, 2018), separately processing top-down and bottom-up error signals to update inference estimates (Figure 11, Left). While some empirical support for amortization exists (Yildirim et al., 2015; Dasgupta et al., 2018), further investigation is needed. Finally, this perspective implies separate computational processing for prediction and inference, with distinct (but linked) frequencies. While some evidence supports this conjecture (Bastos et al., 2015), it is unclear how this could be implemented in biological neurons.

Backpropagation   The biological plausibility of backpropagation is an open question (Lillicrap et al., 2020). Critics argue that backpropagation requires non-local learning signals (Grossberg, 1987; Crick, 1989), whereas the brain relies largely on local learning rules (Hebb, 1949; Markram et al., 1997; Bi & Poo, 1998). "Biologically-plausible" formulations of backpropagation have been proposed (Stork, 1989; Körding & König, 2001; Xie & Seung, 2003; Hinton, 2007; Lillicrap et al., 2016), attempting to reconcile this disparity.

Yet, consensus is still lacking. From another perspective, the apparent biological implausibility of backpropagation may instead be the result of incorrectly assuming a one-to-one correspondence between biological and artificial neurons.

Placing deep networks in correspondence with pyramidal neurons suggests a different perspective on the biological-plausibility debate. In hierarchical latent variable models, prediction errors at each level provide a local learning signal (Friston, 2005; Bengio, 2014; Lee et al., 2015; Whittington & Bogacz, 2017). Thus, learning within each latent level is performed through optimization of local errors. This is exemplified by hierarchical VAEs (Sønderby et al., 2016), which utilize backpropagation *within* each latent level, but not *across* levels. This suggests that learning *within* pyramidal neurons may be more analogous to backpropagation (Figure 12). One possible candidate is backpropagating action potentials (G. J. Stuart & Sakmann, 1994; Williams & Stuart, 2000), which actively propagate a signal of neural activity back to synaptic inputs (G. Stuart et al., 1997; Brunner & Szabadics, 2016), resulting in a variety of synaptic changes throughout the dendrites (Johenning et al., 2015). While computational models from Schiess et al. (2016) support this conjecture, further investigation is needed.

6.2   Lateral Inhibition & Normalizing Flows

Sensory Input Normalization   One of the key computational roles of early sensory areas appears to be reducing spatiotemporal redundancies, i.e., normalization. In retina, this is performed through lateral inhibition via horizontal and amacrine cells, removing correlations (Graham et al., 2006; Pitkow & Meister, 2012). Normalization and prediction are inseparable, and, accordingly, previous works have framed early sensory processing in terms of spatiotemporal predictive coding (Srinivasan et al., 1982; Hosoya et al., 2005; Palmer et al., 2015). This is often motivated in terms of increased sensitivity or efficiency (Srinivasan et al., 1982; Atick & Redlich, 1990) due to redundancy reduction (Barlow et al., 1961, 1989), i.e., compression.

If we consider cortex as a hierarchical latent variable model, then early sensory areas are implicated in parameterizing the conditional likelihood. The ubiquity of normalization in these areas is suggestive of normalization in a flow-based model, implementing the inference direction of a flow-based conditional likelihood (Agrawal & Dukkipati, 2016; Winkler et al., 2019). In addition to the sensitivity and efficiency benefits cited above, this learned, normalized space simplifies downstream generative modeling and improves generalization (Marino et al., 2020).

Normalization in Thalamus   Normalization also appears to occur in first-order thalamic relays, such as the lateral geniculate nucleus (LGN). Dong & Atick (1995) framed LGN in terms of temporal normalization, with supporting evidence provided by Dan et al. (1996). This has the effect of removing predictable temporal structure, e.g., static backgrounds. Under the interpretation above, this is an additional inference stage of a flow-based conditional likelihood (Marino et al., 2020).
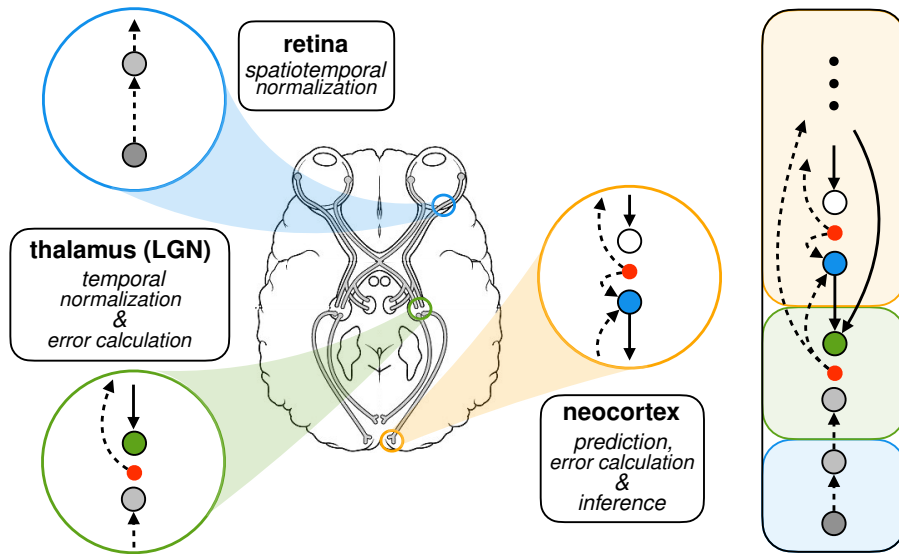
Figure 13: **Visual Pathway**. Retina and LGN are interpreted as implementing normalizing flows, i.e., spatiotemporal predictive coding, reducing spatial and temporal redundancy in the visual input (dashed arrows between gray circles). LGN is also the lowest level for hierarchical predictions from cortex. Using prediction errors throughout the hierarchy, forward cortical connections update latent estimates.

Normalization in Cortex Normalization, via local lateral inhibition, is also found throughout cortex (King et al., 2013). Friston (2005) suggested that this plays the role of inverse covariance (precision) matrices, modeling dependencies between dimensions within the same latent level of the hierarchy. This corresponds to parameterizing approximate posteriors (Rezende & Mohamed, 2015; Kingma et al., 2016) and/or conditional priors (C.-W. Huang et al., 2017) with affine normalizing flows with linear dependencies.[5] Normalizing flows offers a more general framework for describing these computations. Further, Friston (2005) assumes that these dependencies are modeled using *symmetric* weights, whereas normalizing flows permits *non-symmetric* schemes, e.g., using autoregressive models (Kingma et al., 2016) or ensembles (Uria et al., 2014). These weights can also be restricted to local spatial regions (Vahdat & Kautz, 2020). Similar normalization operations can also parameterize temporal dynamics (Marino et al., 2020), akin to Friston's generalized coordinates (Friston, 2008a). The overall computational scheme is shown in Figure 13.

---

[5] Specifically, Friston (2005) employs zero-phase component analysis (ZCA) whitening, whereas Kingma et al. (2016) explored Cholesky whitening.

7 Discussion

We have reviewed predictive coding and VAEs, identifying their shared history and formulations. These connections provide an invaluable link between leading areas of theoretical neuroscience and machine learning, hopefully facilitating the transfer of ideas across fields. We have initiated this process by proposing two novel correspondences suggested by this perspective: 1) dendrites of pyramidal neurons and deep networks, and 2) lateral inhibition and normalizing flows. Placing pyramidal neurons in correspondence with deep networks departs from the traditional one-to-one analogy of biological and artificial neurons, raising questions regarding dendritic computation and backpropagation. Normalizing flows offers a more general framework for normalization via lateral inhibition. Connecting these areas may provide new insights for both machine learning and neuroscience, helping us move beyond overly simplistic comparisons.

Predictive Coding → **VAEs** Although considerable independent progress has recently occurred in VAEs, such models are often still trained on relatively simple, standardized datasets of static images. Thus, predictive coding and neuroscience may still hold insights for improving these models for real-world settings. For instance, the correspondences outlined above may offer new architectural insights in designing deep networks and normalizing flows, e.g., drawing on dendritic morphology, short-term plasticity, and connectivity. Predictive coding has also used prediction precision as a form of attention (Feldman & Friston, 2010). More broadly, neuroscience may provide insights into interfacing VAEs with other computations, as well as within embodied agents.

VAEs → **Predictive Coding** Another motivating factor in connecting these areas stems from a desire for large-scale, testable models of predictive coding. While predictive coding offers general considerations for neural activity, e.g., predictions, prediction errors, and extra-classical receptive fields (Rao & Ballard, 1999), it is difficult to align such hypotheses with real data due to the many possible design choices (Gershman, 2019). Current models are often implemented in simplified settings, with few, if any, learned parameters. VAEs, in contrast, offer a large-scale test-bed for implementing models and evaluating them on natural stimuli. This may offer a more nuanced perspective over current efforts to compare biological and artificial neural activity (Yamins et al., 2014).

While we have reviewed many topics across neuroscience and machine learning, for brevity, we have focused exclusively on passive perceptual settings. However, separate, growing bodies of work are incorporating predictive coding (Adams et al., 2013) and VAEs (Ha & Schmidhuber, 2018) within active settings, e.g., reinforcement learning. We are hopeful that the connections in this paper will inspire further insight in such areas.

References

Ackley, D. H., Hinton, G. E., & Sejnowski, T. J. (1985). A learning algorithm for boltzmann machines. *Cognitive science*, *9*(1), 147–169.

Adams, R. A., Shipp, S., & Friston, K. J. (2013). Predictions not commands: active inference in the motor system. *Brain Structure and Function*, *218*(3), 611–643.

Agrawal, S., & Dukkipati, A. (2016). Deep variational inference without pixel-wise reconstruction. *arXiv preprint arXiv:1611.05209*.

Alemi, A., Poole, B., Fischer, I., Dillon, J., Saurous, R. A., & Murphy, K. (2018). Fixing a broken elbo. In *International conference on machine learning* (pp. 159–168).

Alink, A., Schwiedrzik, C. M., Kohler, A., Singer, W., & Muckli, L. (2010). Stimulus predictability reduces responses in primary visual cortex. *Journal of Neuroscience*, *30*(8), 2960–2966.

Andrychowicz, M., Denil, M., Gomez, S., Hoffman, M. W., Pfau, D., Schaul, T., & de Freitas, N. (2016). Learning to learn by gradient descent by gradient descent. In *Advances in neural information processing systems (nips)* (pp. 3981–3989).

Ashby, W. R. (1956). *An introduction to cybernetics*. Chapman and Hall.

Atal, B., & Schroeder, M. (1979). Predictive coding of speech signals and subjective error criteria. *IEEE Transactions on Acoustics, Speech, and Signal Processing*, *27*(3), 247–254.

Atick, J. J., & Redlich, A. N. (1990). Towards a theory of early visual processing. *Neural computation*, *2*(3), 308–320.

Atick, J. J., & Redlich, A. N. (1992). What does the retina know about natural scenes? *Neural computation*, *4*(2), 196–210.

Baccus, S. A., Ölveczky, B. P., Manu, M., & Meister, M. (2008). A retinal circuit that computes object motion. *Journal of Neuroscience*, *28*(27), 6807–6817.

Ballard, D. H. (1987). Modular learning in neural networks. In *Aaai* (pp. 279–284).

Barlow, H. B. (1961). The coding of sensory messages. *Current problems in animal behavior*.

Barlow, H. B. (1989). Unsupervised learning. *Neural computation*, *1*(3), 295–311.

Barlow, H. B., Kaushal, T. P., & Mitchison, G. J. (1989). Finding minimum entropy codes. *Neural Computation*, *1*(3), 412–423.

Barlow, H. B., et al. (1961). Possible principles underlying the transformation of sensory messages. *Sensory communication*, *1*, 217–234.

Bastos, A. M., Usrey, W. M., Adams, R. A., Mangun, G. R., Fries, P., & Friston, K. (2012). Canonical microcircuits for predictive coding. *Neuron*, *76*(4), 695–711.

Bastos, A. M., Vezoli, J., Bosman, C. A., Schoffelen, J.-M., Oostenveld, R., Dowdall, J. R., . . . Fries, P. (2015). Visual areas exert feedforward and feedback influences through distinct frequency channels. *Neuron*, *85*(2), 390–401.

Bekkers, J. M. (2011). Pyramidal neurons. *Current Biology*, *21*(24), R975.

Bell, A. J., & Sejnowski, T. J. (1997). The "independent components" of natural scenes are edge filters. *Vision research*, *37*(23), 3327–3338.

Bengio, Y. (2014). How auto-encoders could provide credit assignment in deep networks via target propagation. *arXiv preprint arXiv:1407.7906*.

Bengio, Y., & Bengio, S. (2000). Modeling high-dimensional discrete data with multi-layer neural networks. In *Advances in neural information processing systems* (pp. 400–406).

Beniaguev, D., Segev, I., & London, M. (2021). Single cortical neurons as deep artificial neural networks. *Neuron*.

Bi, G.-q., & Poo, M.-m. (1998). Synaptic modifications in cultured hippocampal neurons: dependence on spike timing, synaptic strength, and postsynaptic cell type. *Journal of neuroscience*, *18*(24), 10464–10472.

Bialek, W., Rieke, F., Van Steveninck, R. D. R., & Warland, D. (1991). Reading a neural code. *Science*, *252*(5014), 1854–1857.

Brunner, J., & Szabadics, J. (2016). Analogue modulation of back-propagating action potentials enables dendritic hybrid signalling. *Nature communications*, *7*, 13033.

Carandini, M., & Heeger, D. J. (2012). Normalization as a canonical neural computation. *Nature Reviews Neuroscience*, *13*(1), 51–62.

Chen, S. S., & Gopinath, R. A. (2001). Gaussianization. In *Advances in neural information processing systems* (pp. 423–429).

Child, R. (2020). Very deep vaes generalize autoregressive models and can outperform them on images. *arXiv preprint arXiv:2011.10650*.

Chua, K., Calandra, R., McAllister, R., & Levine, S. (2018). Deep reinforcement learning in a handful of trials using probabilistic dynamics models. In *Advances in neural information processing systems* (pp. 4754–4765).

Chung, J., Kastner, K., Dinh, L., Goel, K., Courville, A. C., & Bengio, Y. (2015). A recurrent latent variable model for sequential data. In *Advances in neural information processing systems* (pp. 2980–2988).

Clark, A. (2013). Whatever next? predictive brains, situated agents, and the future of cognitive science. *Behavioral and Brain Sciences*, *36*(3), 181–204.

Comon, P. (1994). Independent component analysis, a new concept? *Signal processing*, *36*(3), 287–314.

Cornish, R., Caterini, A. L., Deligiannidis, G., & Doucet, A. (2020). Relaxing bijectivity constraints with continuously indexed normalising flows. In *International conference on machine learning*.

Covic, E. N., & Sherman, S. M. (2011). Synaptic properties of connections between the primary and secondary auditory cortices in mice. *Cerebral Cortex*, *21*(11), 2425–2441.

Cremer, C., Li, X., & Duvenaud, D. (2018). Inference suboptimality in variational autoencoders. In *International conference on machine learning* (pp. 1078–1086).

Crick, F. (1989). The recent excitement about neural networks. *Nature*, *337*(6203), 129–132.

Dan, Y., Atick, J. J., & Reid, R. C. (1996). Efficient coding of natural scenes in the lateral geniculate nucleus: experimental test of a computational theory. *Journal of Neuroscience*, *16*(10), 3351–3362.

Dasgupta, I., Schulz, E., Goodman, N. D., & Gershman, S. J. (2018). Remembrance of inferences past: Amortization in human hypothesis generation. *Cognition*, *178*, 67–81.

Dayan, P., & Hinton, G. E. (1996). Varieties of helmholtz machine. *Neural Networks*, *9*(8), 1385–1403.

Dayan, P., Hinton, G. E., Neal, R. M., & Zemel, R. S. (1995). The helmholtz machine. *Neural computation*, *7*(5), 889–904.

Deco, G., & Brauer, W. (1995). Higher order statistical decorrelation without information loss. In *Advances in neural information processing systems* (pp. 247–254).

Dempster, A. P., Laird, N. M., & Rubin, D. B. (1977). Maximum likelihood from incomplete data via the em algorithm. *Journal of the royal statistical society. Series B (methodological)*, 1–38.

Deng, J., Dong, W., Socher, R., Li, L.-J., Li, K., & Fei-Fei, L. (2009). Imagenet: A large-scale hierarchical image database. In *2009 ieee conference on computer vision and pattern recognition* (pp. 248–255).

De Pasquale, R., & Sherman, S. M. (2011). Synaptic properties of corticocortical connections between the primary and secondary visual cortical areas in the mouse. *Journal of Neuroscience*, *31*(46), 16494–16506.

Dinh, L., Krueger, D., & Bengio, Y. (2015). Nice: Non-linear independent components estimation. In *International conference on learning representations.*

Dinh, L., Sohl-Dickstein, J., & Bengio, S. (2017). Density estimation using real nvp. In *International conference on learning representations.*

Dong, D. W., & Atick, J. J. (1995). Temporal decorrelation: a theory of lagged and nonlagged responses in the lateral geniculate nucleus. *Network: Computation in Neural Systems*, *6*(2), 159–178.

Douglas, R. J., Martin, K. A., & Whitteridge, D. (1989). A canonical microcircuit for neocortex. *Neural computation*, *1*(4), 480–488.

Doya, K., Ishii, S., Pouget, A., & Rao, R. P. (2007). *Bayesian brain: Probabilistic approaches to neural coding.* MIT press.

Ebert, F., Finn, C., Lee, A. X., & Levine, S. (2017). Self-supervised visual planning with temporal skip connections. In *Conference on robot learning.*

Egner, T., Monti, J. M., & Summerfield, C. (2010). Expectation and surprise determine neural population responses in the ventral visual stream. *Journal of Neuroscience*, *30*(49), 16601–16608.

Eliades, S. J., & Wang, X. (2008). Neural substrates of vocalization feedback monitoring in primate auditory cortex. *Nature*, *453*(7198), 1102.

Feldman, H., & Friston, K. (2010). Attention, uncertainty, and free-energy. *Frontiers in human neuroscience*, *4*.

Fraccaro, M., Sønderby, S. K., Paquet, U., & Winther, O. (2016). Sequential neural models with stochastic layers. In *Advances in neural information processing systems* (pp. 2199–2207).

Frey, B. J., Hinton, G. E., & Dayan, P. (1996). Does the wake-sleep algorithm produce good density estimators? In *Advances in neural information processing systems* (pp. 661–667).

Friston, K. (2005). A theory of cortical responses. *Philosophical Transactions of the Royal Society of London B: Biological Sciences*, *360*(1456), 815–836.

Friston, K. (2008a). Hierarchical models in the brain. *PLoS computational biology*, *4*(11), e1000211.

Friston, K. (2008b). Variational filtering. *NeuroImage*, *41*(3), 747–766.

Friston, K. (2009). The free-energy principle: a rough guide to the brain? *Trends in cognitive sciences*, *13*(7), 293–301.

Friston, K. (2018). Does predictive coding have a future? *Nature neuroscience*, *21*(8), 1019.

Friston, K., Mattout, J., Trujillo-Barreto, N., Ashburner, J., & Penny, W. (2007). Variational free energy and the laplace approximation. *Neuroimage*, *34*(1), 220–234.

Gershman, S. (2019). What does the free energy principle tell us about the brain? *arXiv preprint arXiv:1901.07945*.

Gershman, S., & Goodman, N. (2014). Amortized inference in probabilistic reasoning. In *Proceedings of the cognitive science society* (Vol. 36).

Gidon, A., Zolnik, T. A., Fidzinski, P., Bolduan, F., Papoutsi, A., Poirazi, P., ... Larkum, M. E. (2020). Dendritic action potentials and computation in human layer 2/3 cortical neurons. *Science*.

Gilbert, C. D., & Sigman, M. (2007). Brain states: top-down influences in sensory processing. *Neuron*, *54*(5), 677–696.

Gillon, C. J., Pina, J. E., Lecoq, J. A., Ahmed, R., Billeh, Y., Caldejon, S., ... others (2021). Learning from unexpected events in the neocortical microcircuit. *bioRxiv*.

Girard, P., & Bullier, J. (1989). Visual activity in area v2 during reversible inactivation of area 17 in the macaque monkey. *Journal of neurophysiology*, *62*(6), 1287–1302.

Girard, P., Salin, P., & Bullier, J. (1991). Visual activity in areas v3a and v3 during reversible inactivation of area v1 in the macaque monkey. *Journal of Neurophysiology*, *66*(5), 1493–1503.

Goodfellow, I., Bengio, Y., & Courville, A. (2016). *Deep learning*. MIT press.

Graham, D. J., Chandler, D. M., & Field, D. J. (2006). Can the theory of "whitening" explain the center-surround properties of retinal ganglion cell receptive fields? *Vision research*, *46*(18), 2901–2913.

Graves, A. (2013). Generating sequences with recurrent neural networks. *arXiv preprint arXiv:1308.0850*.

Gregor, K., Danihelka, I., Mnih, A., Blundell, C., & Wierstra, D. (2014). Deep autoregressive networks. In *Proceedings of the international conference on machine learning (icml)* (pp. 1242–1250).

Gresele, L., Fissore, G., Javaloy, A., Schölkopf, B., & Hyvarinen, A. (2020). Relative gradient optimization of the jacobian term in unsupervised deep learning. *Advances in Neural Information Processing Systems*, *33*.

Grossberg, S. (1987). Competitive learning: From interactive activation to adaptive resonance. *Cognitive science*, *11*(1), 23–63.

Guergiuev, J., Lillicrap, T. P., & Richards, B. A. (2016). Biologically feasible deep learning with segregated dendrites. *arXiv preprint arXiv:1610.00161*.

Gulrajani, I., Kumar, K., Ahmed, F., Taiga, A. A., Visin, F., Vazquez, D., & Courville, A. (2017). Pixelvae: A latent variable model for natural images. In *International conference on learning representations.*

Ha, D., & Schmidhuber, J. (2018). Recurrent world models facilitate policy evolution. In *Advances in neural information processing systems* (pp. 2450–2462).

Hafner, D., Lillicrap, T., Fischer, I., Villegas, R., Ha, D., Lee, H., & Davidson, J. (2019). Learning latent dynamics for planning from pixels. In *International conference on machine learning* (pp. 2555–2565).

Harrison, C. (1952). Experiments with linear prediction in television. *Bell System Technical Journal*, *31*(4), 764–783.

Hawkins, J., & Blakeslee, S. (2004). *On intelligence: How a new understanding of the brain will lead to the creation of truly intelligent machines*. Macmillan.

Hebb, D. O. (1949). The organization of behavior; a neuropsycholocigal theory. *A Wiley Book in Clinical Psychology.*, 62–78.

Higgins, I., Matthey, L., Pal, A., Burgess, C., Glorot, X., Botvinick, M., . . . Lerchner, A. (2017). beta-vae: Learning basic visual concepts with a constrained variational framework. In *Proceedings of the international conference on learning representations (iclr).*

Hinton, G. E. (2007). How to do backpropagation in a brain. *NeurIPS Deep Learning Workshop*.

Hinton, G. E., & Van Camp, D. (1993). Keeping the neural networks simple by minimizing the description length of the weights. In *Proceedings of the sixth annual conference on computational learning theory* (pp. 5–13).

Hjelm, D., Salakhutdinov, R. R., Cho, K., Jojic, N., Calhoun, V., & Chung, J. (2016). Iterative refinement of the approximate posterior for directed belief networks. In *Advances in neural information processing systems (nips)* (pp. 4691–4699).

Hopfield, J. J. (1982). Neural networks and physical systems with emergent collective computational abilities. *Proceedings of the national academy of sciences*, *79*(8), 2554–2558.

Hosoya, T., Baccus, S. A., & Meister, M. (2005). Dynamic predictive coding by the retina. *Nature*, *436*(7047), 71.

Huang, C.-W., Touati, A., Dinh, L., Drozdzal, M., Havaei, M., Charlin, L., & Courville, A. (2017). Learnable explicit density for continuous latent space and variational inference. *arXiv preprint arXiv:1710.02248*.

Huang, Y., & Rao, R. P. (2011). Predictive coding. *Wiley Interdisciplinary Reviews: Cognitive Science*, *2*(5), 580–593.

Hyvärinen, A., & Oja, E. (2000). Independent component analysis: algorithms and applications. *Neural networks*, *13*(4-5), 411–430.

Isaacson, J. S., & Scanziani, M. (2011). How inhibition shapes cortical activity. *Neuron*, *72*(2), 231–243.

Jehee, J. F., & Ballard, D. H. (2009). Predictive feedback can account for biphasic responses in the lateral geniculate nucleus. *PLoS Comput Biol*, *5*(5), e1000373.

Johenning, F. W., Theis, A.-K., Pannasch, U., Rückl, M., Rüdiger, S., & Schmitz, D. (2015). Ryanodine receptor activation induces long-term plasticity of spine calcium dynamics. *PLoS biology*, *13*(6), e1002181.

Jones, I. S., & Kording, K. P. (2020). Can single neurons solve mnist? the computational power of biological dendritic trees. *arXiv preprint arXiv:2009.01269*.

Jordan, M. I., Ghahramani, Z., Jaakkola, T. S., & Saul, L. K. (1998). An introduction to variational methods for graphical models. *NATO ASI SERIES D BEHAVIOURAL AND SOCIAL SCIENCES*, *89*, 105–162.

Kalman, R. E. (1960). A new approach to linear filtering and prediction problems. *Journal of Basic Engineering*, *82*(1), 35–45.

Kanai, R., Komura, Y., Shipp, S., & Friston, K. (2015). Cerebral hierarchies: predictive processing, precision and the pulvinar. *Phil. Trans. R. Soc. B*, *370*(1668), 20140169.

Keller, G. B., Bonhoeffer, T., & Hübener, M. (2012). Sensorimotor mismatch signals in primary visual cortex of the behaving mouse. *Neuron*, *74*(5), 809–815.

Keller, G. B., & Mrsic-Flogel, T. D. (2018). Predictive processing: a canonical cortical computation. *Neuron*, *100*(2), 424–435.

Kessy, A., Lewin, A., & Strimmer, K. (2018). Optimal whitening and decorrelation. *The American Statistician*, *72*(4), 309–314.

Khemakhem, I., Kingma, D., Monti, R., & Hyvarinen, A. (2020). Variational autoencoders and nonlinear ica: A unifying framework. In *International conference on artificial intelligence and statistics* (pp. 2207–2217).

Kim, Y., Wiseman, S., Miller, A. C., Sontag, D., & Rush, A. M. (2018). Semi-amortized variational autoencoders. In *Proceedings of the international conference on machine learning (icml).*

King, P. D., Zylberberg, J., & DeWeese, M. R. (2013). Inhibitory interneurons decorrelate excitatory cells to drive sparse code formation in a spiking model of v1. *Journal of Neuroscience*.

Kingma, D. P., Salimans, T., Jozefowicz, R., Chen, X., Sutskever, I., & Welling, M. (2016). Improved variational inference with inverse autoregressive flow. In *Advances in neural information processing systems* (pp. 4743–4751).

Kingma, D. P., & Welling, M. (2014). Stochastic gradient vb and the variational auto-encoder. In *Proceedings of the international conference on learning representations.*

Körding, K. P., & König, P. (2001). Supervised and unsupervised learning with two sites of synaptic integration. *Journal of computational neuroscience*, *11*(3), 207–215.

Krishnan, R. G., Liang, D., & Hoffman, M. (2018). On the challenges of learning with inference networks on sparse, high-dimensional data. In *Proceedings of the international conference on artificial intelligence and statistics (aistats)* (pp. 143–151).

Kumar, M., Babaeizadeh, M., Erhan, D., Finn, C., Levine, S., Dinh, L., & Kingma, D. P. (2020). Videoflow: A flow-based generative model for video. In *International conference on learning representations.*

Laparra, V., Camps-Valls, G., & Malo, J. (2011). Iterative gaussianization: from ica to random rotations. *IEEE transactions on neural networks*, *22*(4), 537–549.

Laughlin, S. (1981). A simple coding procedure enhances a neuron's information capacity. *Zeitschrift für Naturforschung c*, *36*(9-10), 910–912.

LeCun, Y., Bengio, Y., & Hinton, G. E. (2015). Deep learning. *nature*, *521*(7553), 436–444.

Lee, D.-H., Zhang, S., Fischer, A., & Bengio, Y. (2015). Difference target propagation. In *Joint european conference on machine learning and knowledge discovery in databases* (pp. 498–515).

Lillicrap, T. P., Cownden, D., Tweed, D. B., & Akerman, C. J. (2016). Random synaptic feedback weights support error backpropagation for deep learning. *Nature communications*, *7*, 13276.

Lillicrap, T. P., Santoro, A., Marris, L., Akerman, C. J., & Hinton, G. (2020). Backpropagation and the brain. *Nature Reviews Neuroscience*, 1–12.

London, M., & Häusser, M. (2005). Dendritic computation. *Annu. Rev. Neurosci.*, *28*, 503–532.

Lotter, W., Kreiman, G., & Cox, D. (2017). Deep predictive coding networks for video prediction and unsupervised learning. In *International conference on learning representations*.

Lotter, W., Kreiman, G., & Cox, D. (2018). A neural network trained to predict future video frames mimics critical properties of biological neuronal responses and perception. *arXiv preprint arXiv:1805.10734*.

Maaløe, L., Fraccaro, M., Lievin, V., & Winther, O. (2019). Biva: A very deep hierarchy of latent variables for generative modeling. In *Advances in neural information processing systems* (p. 8882).

MacKay, D. M. (1956). The epistemological problem for automata. *Automata studies*, 235–252.

Marino, J., Chen, L., He, J., & Mandt, S. (2020). Improving sequential latent variable models with autoregressive flows. In *Symposium on advances in approximate bayesian inference* (pp. 1–16).

Marino, J., Cvitkovic, M., & Yue, Y. (2018). A general method for amortizing variational filtering. In *Advances in neural information processing systems* (pp. 7857–7868).

Marino, J., Yue, Y., & Mandt, S. (2018). Iterative amortized inference. In *International conference on machine learning* (pp. 3403–3412).

Markram, H., Lübke, J., Frotscher, M., & Sakmann, B. (1997). Regulation of synaptic efficacy by coincidence of postsynaptic aps and epsps. *Science*, *275*(5297), 213–215.

McCulloch, W. S., & Pitts, W. (1943). A logical calculus of the ideas immanent in nervous activity. *The bulletin of mathematical biophysics*, *5*(4), 115–133.

Mel, B. W. (1992). The clusteron: toward a simple abstraction for a complex neuron. In *Advances in neural information processing systems*.

Meyer, H. S., Schwarz, D., Wimmer, V. C., Schmitt, A. C., Kerr, J. N., Sakmann, B., & Helmstaedter, M. (2011). Inhibitory interneurons in a cortical column form hot zones of inhibition in layers 2 and 5a. *Proceedings of the National Academy of Sciences*, *108*(40), 16807–16812.

Meyer, T., & Olson, C. R. (2011). Statistical learning of visual transitions in monkey inferotemporal cortex. *Proceedings of the National Academy of Sciences*, *108*(48), 19401–19406.

Mnih, A., & Gregor, K. (2014). Neural variational inference and learning in belief networks. In *International conference on machine learning* (pp. 1791–1799).

Mountcastle, V., Berman, A., & Davies, P. (1955). Topographic organization and modality representation in first somatic area of cat's cerebral cortex by method of single unit analysis. *Am J Physiol*, *183*(464), 10.

Mumford, D. (1991). On the computational architecture of the neocortex. *Biological cybernetics*, *65*(2), 135–145.

Mumford, D. (1992). On the computational architecture of the neocortex. *Biological cybernetics*, *66*(3), 241–251.

Murphy, K. P. (2012). *Machine learning: a probabilistic perspective*. MIT press.

Murray, S. O., Kersten, D., Olshausen, B. A., Schrater, P., & Woods, D. L. (2002). Shape perception reduces activity in human primary visual cortex. *Proceedings of the National Academy of Sciences*, *99*(23), 15164–15169.

Neal, R. M., & Hinton, G. E. (1998). A view of the em algorithm that justifies incremental, sparse, and other variants. In *Learning in graphical models* (pp. 355–368). Springer.

Oliver, B. (1952). Efficient coding. *The Bell System Technical Journal*, *31*(4), 724–750.

Olshausen, B. A., & Field, D. J. (1996). Emergence of simple-cell receptive field properties by learning a sparse code for natural images. *Nature*, *381*(6583), 607.

Olshausen, B. A., & Field, D. J. (1997). Sparse coding with an overcomplete basis set: A strategy employed by v1? *Vision research*, *37*(23), 3311–3325.

Ölveczky, B. P., Baccus, S. A., & Meister, M. (2003). Segregation of object and background motion in the retina. *Nature*, *423*(6938), 401–408.

Palmer, S. E., Marre, O., Berry, M. J., & Bialek, W. (2015). Predictive information in a sensory population. *Proceedings of the National Academy of Sciences*, *112*(22), 6908–6913.

Papamakarios, G., Pavlakou, T., & Murray, I. (2017). Masked autoregressive flow for density estimation. In *Advances in neural information processing systems* (pp. 2338–2347).

Park, Y., Kim, C., & Kim, G. (2019). Variational laplace autoencoders. In *International conference on machine learning* (pp. 5032–5041).

Parra, L., Deco, G., & Miesbach, S. (1995). Redundancy reduction with information-preserving nonlinear maps. *Network: Computation in Neural Systems*, *6*(1), 61–72.

Parras, G. G., Nieto-Diego, J., Carbajal, G. V., Valdés-Baizabal, C., Escera, C., & Malmierca, M. S. (2017). Neurons along the auditory pathway exhibit a hierarchical organization of prediction error. *Nature communications*, *8*(1), 1–17.

Pearl, J. (1986). Fusion, propagation, and structuring in belief networks. *Artificial Intelligence*, *29*(3), 241–288.

Pitkow, X., & Meister, M. (2012). Decorrelation and efficient coding by retinal ganglion cells. *Nature neuroscience*, *15*(4), 628.

Poirazi, P., Brannon, T., & Mel, B. W. (2003). Pyramidal neuron as two-layer neural network. *Neuron*, *37*(6), 989–999.

Polsky, A., Mel, B. W., & Schiller, J. (2004). Computational subunits in thin dendrites of pyramidal cells. *Nature neuroscience*, *7*(6), 621.

Pourahmadi, M. (2011). Covariance estimation: The glm and regularization perspectives. *Statistical Science*, 369–387.

Prieto, A., Prieto, B., Ortigosa, E. M., Ros, E., Pelayo, F., Ortega, J., & Rojas, I. (2016). Neural networks: An overview of early research, current frameworks and new challenges. *Neurocomputing*, *214*, 242–268.

Radford, A., Wu, J., Child, R., Luan, D., Amodei, D., & Sutskever, I. (2019). Language models are unsupervised multitask learners.

Rao, R. P. (1998). Correlates of attention in a model of dynamic visual recognition. In *Advances in neural information processing systems* (pp. 80–86).

Rao, R. P., & Ballard, D. H. (1999). Predictive coding in the visual cortex: a functional interpretation of some extra-classical receptive-field effects. *Nature neuroscience*, *2*(1).

Rao, R. P., & Sejnowski, T. J. (2002). Predictive coding, cortical feedback, and spike-timing dependent plasticity. *Probabilistic models of the brain*, 297.

Razavi, A., van den Oord, A., & Vinyals, O. (2019). Generating diverse high-fidelity images with vq-vae-2. In *Advances in neural information processing systems* (pp. 14866–14876).

Rezende, D. J., & Mohamed, S. (2015). Variational inference with normalizing flows. In *International conference on machine learning* (pp. 1530–1538).

Rezende, D. J., Mohamed, S., & Wierstra, D. (2014). Stochastic backpropagation and approximate inference in deep generative models. In *Proceedings of the international conference on machine learning* (pp. 1278–1286).

Rezende, D. J., & Viola, F. (2018). Taming vaes. *arXiv preprint arXiv:1810.00597*.

Rippel, O., & Adams, R. P. (2013). High-dimensional probability estimation with deep density models. *arXiv preprint arXiv:1302.5125*.

Rosenblatt, F. (1958). The perceptron: a probabilistic model for information storage and organization in the brain. *Psychological review*, *65*(6), 386.

Rumelhart, D. E., Hinton, G. E., & Williams, R. J. (1986). Learning representations by back-propagating errors. *Nature*.

Schiess, M., Urbanczik, R., & Senn, W. (2016). Somato-dendritic synaptic plasticity and error-backpropagation in active dendrites. *PLoS computational biology*, *12*(2), e1004638.

Schmidhuber, J. (2015). Deep learning in neural networks: An overview. *Neural networks*, *61*, 85–117.

Shannon, C. E. (1948). A mathematical theory of communication. *The Bell system technical journal*, *27*(3), 379–423.

Sharma, J., Angelucci, A., & Sur, M. (2000). Induction of visual orientation modules in auditory cortex. *Nature*, *404*(6780), 841.

Sherman, S. M., & Guillery, R. (2002). The role of the thalamus in the flow of information to the cortex. *Philosophical Transactions of the Royal Society of London. Series B: Biological Sciences*, *357*(1428), 1695–1708.

Sønderby, C. K., Raiko, T., Maaløe, L., Sønderby, S. K., & Winther, O. (2016). Ladder variational autoencoders. In *Advances in neural information processing systems (nips)* (pp. 3738–3746).

Spratling, M. W. (2008). Reconciling predictive coding and biased competition models of cortical function. *Frontiers in computational neuroscience*, *2*, 4.

Srinivasan, M. V., Laughlin, S., & Dubs, A. (1982). Predictive coding: a fresh view of inhibition in the retina. *Proceedings of the Royal Society of London. Series B. Biological Sciences*, *216*(1205), 427–459.

Stork, D. G. (1989). Is backpropagation biologically plausible. In *International joint conference on neural networks* (Vol. 2, pp. 241–246).

Stuart, G., Spruston, N., Sakmann, B., & Häusser, M. (1997). Action potential initiation and backpropagation in neurons of the mammalian cns. *Trends in neurosciences*, *20*(3), 125–131.

Stuart, G. J., & Sakmann, B. (1994). Active propagation of somatic action potentials into neocortical pyramidal cell dendrites. *Nature*, *367*(6458), 69.

Summerfield, C., Egner, T., Greene, M., Koechlin, E., Mangels, J., & Hirsch, J. (2006). Predictive codes for forthcoming perception in the frontal cortex. *Science*, *314*(5803), 1311–1314.

Sutskever, I., Vinyals, O., & Le, Q. V. (2014). Sequence to sequence learning with neural networks. In *Advances in neural information processing systems* (pp. 3104–3112).

Tabak, E. G., & Turner, C. V. (2013). A family of nonparametric density estimation algorithms. *Communications on Pure and Applied Mathematics*, *66*(2), 145–164.

Tipping, M. E., & Bishop, C. M. (1999). Probabilistic principal component analysis. *Journal of the Royal Statistical Society: Series B (Statistical Methodology)*, *61*(3), 611–622.

Uria, B., Murray, I., & Larochelle, H. (2014). A deep and tractable density estimator. In *International conference on machine learning* (pp. 467–475).

Vahdat, A., & Kautz, J. (2020). Nvae: A deep hierarchical variational autoencoder. *Advances in Neural Information Processing Systems*, *33*.

van den Broeke, G. (2016). *What auto-encoders could learn from brains* (Unpublished master's thesis). Aalto University.

van den Oord, A., Dieleman, S., Zen, H., Simonyan, K., Vinyals, O., Graves, A., ... Kavukcuoglu, K. (2016). Wavenet: A generative model for raw audio. In *9th isca speech synthesis workshop* (pp. 125–125).

van den Oord, A., Kalchbrenner, N., & Kavukcuoglu, K. (2016). Pixel recurrent neural networks. In *International conference on machine learning* (pp. 1747–1756).

van den Oord, A., Li, Y., Babuschkin, I., Simonyan, K., Vinyals, O., Kavukcuoglu, K., ... others (2018). Parallel wavenet: Fast high-fidelity speech synthesis. In *International conference on machine learning* (pp. 3915–3923).

Van Essen, D. C., & Maunsell, J. H. (1983). Hierarchical organization and functional streams in the visual cortex. *Trends in neurosciences*, *6*, 370–375.

Von Helmholtz, H. (1867). *Handbuch der physiologischen optik* (Vol. 9). Voss.

Wacongne, C., Labyt, E., van Wassenhove, V., Bekinschtein, T., Naccache, L., & Dehaene, S. (2011). Evidence for a hierarchy of predictions and prediction errors in human cortex. *Proceedings of the National Academy of Sciences*, *108*(51), 20754–20759.

Walsh, K. S., McGovern, D. P., Clark, A., & O'Connell, R. G. (2020). Evaluating the neurophysiological evidence for predictive processing as a model of perception. *Annals of the New York Academy of Sciences*, *1464*(1), 242.

Whittington, J. C., & Bogacz, R. (2017). An approximation of the error backpropagation algorithm in a predictive coding network with local hebbian synaptic plasticity. *Neural computation*.

Widrow, B., & Hoff, M. E. (1960). *Adaptive switching circuits* (Tech. Rep.). Stanford Univ Ca Stanford Electronics Labs.

Wiegand, T., Sullivan, G. J., Bjontegaard, G., & Luthra, A. (2003). Overview of the h. 264/avc video coding standard. *IEEE Transactions on circuits and systems for video technology*, *13*(7), 560–576.

Wiener, N. (1942). *The interpolation, extrapolation and smoothing of stationary time series. ndrc report.* Cambridge. Wiley, New York.

Wiener, N. (1948). *Cybernetics or control and communication in the animal and the machine*. MIT press.

Williams, S. R., & Stuart, G. J. (2000). Backpropagation of physiological spike trains in neocortical pyramidal neurons: implications for temporal coding in dendrites. *Journal of Neuroscience*.

Winkler, C., Worrall, D., Hoogeboom, E., & Welling, M. (2019). Learning likelihoods with conditional normalizing flows. *arXiv preprint arXiv:1912.00042*.

Xie, X., & Seung, H. S. (2003). Equivalence of backpropagation and contrastive hebbian learning in a layered network. *Neural computation*, *15*(2), 441–454.

Yamins, D. L., Hong, H., Cadieu, C. F., Solomon, E. A., Seibert, D., & DiCarlo, J. J. (2014). Performance-optimized hierarchical models predict neural responses in higher visual cortex. *Proceedings of the national academy of sciences*, *111*(23), 8619–8624.

Yildirim, I., Kulkarni, T. D., Freiwald, W. A., & Tenenbaum, J. B. (2015). Efficient and robust analysis-by-synthesis in vision: A computational framework, behavioral tests, and modeling neuronal representations. In *Thirty-seventh annual conference of the cognitive science society* (Vol. 4).

Zador, A. M., Claiborne, B. J., & Brown, T. H. (1992). Nonlinear pattern separation in single hippocampal neurons with active dendritic membrane. In *Advances in neural information processing systems* (pp. 51–58).

Zmarz, P., & Keller, G. B. (2016). Mismatch receptive fields in mouse visual cortex. *Neuron*, *92*(4), 766–772.

A   Variational Bound Derivation

We can express the KL divergence between $q(\mathbf{z}|\mathbf{x})$ and $p_\theta(\mathbf{z}|\mathbf{x})$ as

$$
\begin{aligned}
D_{\mathrm{KL}}(q(\mathbf{z}|\mathbf{x})||p_\theta(\mathbf{z}|\mathbf{x})) &= \mathbb{E}_{\mathbf{z}\sim q(\mathbf{z}|\mathbf{x})}\left[\log q(\mathbf{z}|\mathbf{x}) - \log p_\theta(\mathbf{z}|\mathbf{x})\right] \\
&= \mathbb{E}_{\mathbf{z}\sim q(\mathbf{z}|\mathbf{x})}\left[\log q(\mathbf{z}|\mathbf{x}) - \log\left(\frac{p_\theta(\mathbf{x},\mathbf{z})}{p_\theta(\mathbf{x})}\right)\right] \\
&= \underbrace{\mathbb{E}_{\mathbf{z}\sim q(\mathbf{z}|\mathbf{x})}\left[\log q(\mathbf{z}|\mathbf{x}) - \log p_\theta(\mathbf{x},\mathbf{z})\right]}_{-\mathcal{L}(\mathbf{x};q,\theta)} + \log p_\theta(\mathbf{x}). \qquad (26)
\end{aligned}
$$